Journal of Medicinal Chemistry

Article

pubs.acs.org/jmc

Synthesis and Biological Evaluation of Direct Thrombin Inhibitors Bearing 4-(Piperidin-1-yl)pyridine at the P1 Position with Potent Anticoagulant Activity

Modesto de Candia,[†] Filomena Fiorella,[†,⊥] Gianfranco Lopopolo,[†,▽] Andrea Carotti,[‡] Maria Rosaria Romano,[†] Marcello Diego Lograno,[†] Sophie Martel,[§] Pierre-Alain Carrupt,[§] Benny D. Belviso,[∥] Rocco Caliandro,[∥] and Cosimo Altomare*,[†]

[†]Dipartimento di Farmacia-Scienze del Farmaco, University of Bari "Aldo Moro", Via E. Orabona 4, 70125 Bari, Italy

[‡]Dipartimento di Chimica e Tecnologia del Farmaco, University of Perugia, Via del Liceo 1, 60123 Perugia, Italy

[§]School of Pharmaceutical Sciences, University of Geneva, University of Lausanne, Quai Ernest-Ansermet 30, CH-1211 Geneva 4, Switzerland

[∥]Istituto di Cristallografia, Consiglio Nazionale delle Ricerche, Via Amendola 122/o, 70126 Bari, Italy

Supporting Information

ABSTRACT: The design and synthesis of a new class of nonpeptide direct thrombin inhibitors, built on the structure of 1-(pyridin-4-yl)piperidine-4-carboxamide, are described. Starting from a strongly basic 1-amidinopiperidine derivative (**6**) showing poor thrombin (fIIa) and factor Xa (fXa) inhibition activities, anti-fIIa activity and artificial membrane permeability were considerably improved by optimizing the basic P1 and the X-substituted phenyl P4 binding moieties. Structure–activity relationship studies, usefully complemented with molecular modeling results, led us to identify compound **13b**, which showed excellent fIIa inhibition (K_i = 6 nM), weak anti-Xa activity (K_i = 5.64 μM), and remarkable selectivity over other serine proteases (e.g., trypsin). Compound **13b** showed in vitro anticoagulant activity in the low micromolar range and significant membrane permeability. In mice (ex vivo), **13b** demonstrated anticoagulant effects at 2 h after oral dosing (100 mg·kg^{-1}), with a significant 43% prolongation of the activated partial thromboplastin time (aPTT), over controls (P < 0.05).

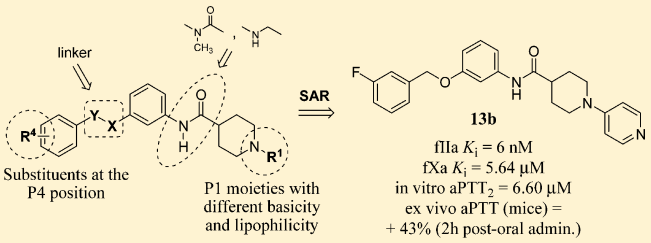

INTRODUCTION

Thrombotic disorders, including deep venous thrombosis (DVT), venous thromboembolism (VTE), pulmonary embolism (PE), myocardial infarction, unstable angina, and stroke, are major causes of morbidity and mortality worldwide, with a higher incidence in developed countries.[1] Current antithrombotic therapies mostly rely on traditional anticoagulants, including vitamin K antagonists and heparins [both unfractionated (UFHs) and low-molecular-weight heparins (LMWHs)].[2] In spite of their proven clinical efficacy, these agents have limitations that restrict their usefulness in therapy.[1] Vitamin K antagonists, such as warfarin, interfering with biosynthesis of coagulation factors (II, VII, IX, X), proteins C and S, have long been the only approved oral anticoagulant treatments,[3] but their use is often associated with considerable shortcomings, such as drug and food interactions, highly variable pharmacokinetics (PK) and pharmacodynamics (PD) profiles, and intra- and interpatient variability in drug response. Warfarin-treated patients need continuous monitoring of clinical coagulation parameters and frequent dose adjustment to avoid bleeding complications.[4] UFHs, LMWHs, and the indirect fXa inhibitor fondaparinux, whose anticoagulant activity is mediated by the inhibition of antithrombin III (ATIII), require parenteral administration, which makes their use outside the hospital difficult. Moreover, UFHs, whose anticoagulant responses need monitoring, are not active against fibrin-bound fIIa, have unpredictable PK profiles, and can trigger formation of antibodies, causing heparin-induced thrombocytopenia (HIT).[2,5] Other parenteral anticoagulants include the direct thrombin inhibitors (DTIs), such as the peptides hirudin and bivalirudin, and argatroban, which is the only synthetic small-molecule DTI currently in use for intravenous administration.[6]

In the search for safer antithrombotic drugs, enzymes (factors) of the blood coagulation cascade, such as fIIa, fXa, and fVIIa, have been identified as drug targets.[7] Thrombin is a trypsin-like serine protease that catalyzes the conversion of soluble fibrinogen into insoluble fibrin in the final step of clot formation and primary hemostasis.[8,9] The thrombin active site features the catalytic triad, formed by Asp102, His57, and Ser195, and four distinct substrate binding sites (S1–S4). The S1 site is a major determinant of substrate specificity; it is a

Received: August 1, 2013

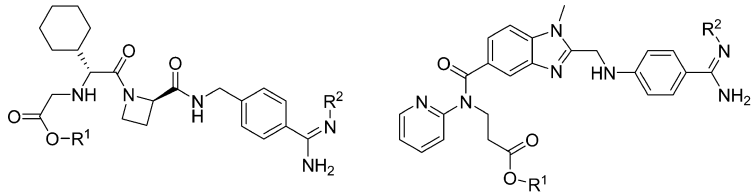

1, $R^1 = R^2 = H$: Melagatran
2, $R^1 = Et$, $R^2 = OH$: Ximelagatran
3, $R^1 = R^2 = H$: Dabigatran
4, $R^1 = Et$, $R^2 = CO_2$-*n*-hexyl: Dabigatran etexilate

Figure 1. Structures of approved oral direct thrombin inhibitors.

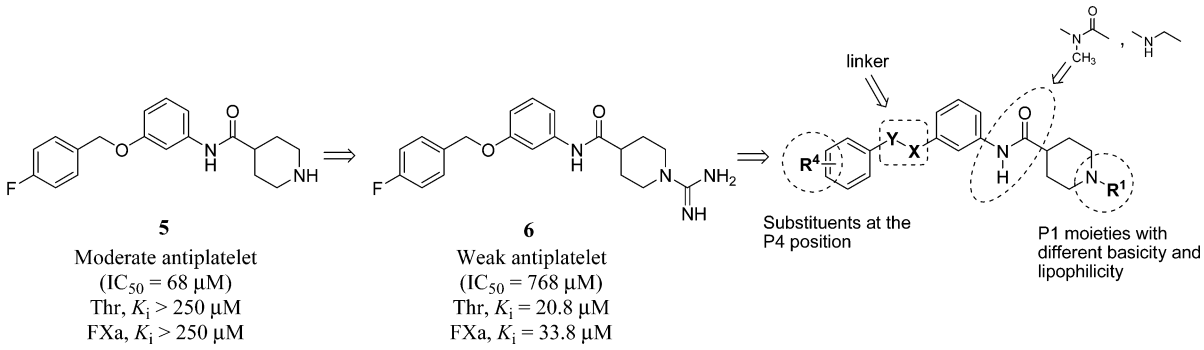

Figure 2. Isonipecotamide-based antithrombotic agents and molecular modification of compound **6** for the SAR study.

deep pocket, mainly hydrophobic, containing the Asp189 residue at the bottom, which shows a preference for the Arg residue in the protein substrate sequence. The proximal S2 pocket in the insertion loop 60A–D (Tyr60A, Pro60B, Pro60C, and Trp60D) accommodates small-size hydrophobic residues in substrate sequence (e.g., Pro). In the flat S3 site, ligands (both substrates and inhibitors) may bind in an antiparallel hydrogen bonding pattern usually involving Gly216 in fIIa. The large hydrophobic S4 site, also called D-pocket (D stands for distal from the catalytic Ser195) or aryl binding site because of its preference for large and aromatic moieties in low-molecular weight ligands, is lined by the hydrophobic residues Leu99, Ile174, and Trp215.[10–12]

In the past decade, extensive efforts have been made to develop direct active-site small-molecule DTIs,[2,3] but despite the large number of discovered potent compounds, only a few DTIs are clinically available. Among them, only one synthetic DTI, argatroban (not shown), is currently in use for intravenous administration in patients with thrombosis and HIT.[13] The first oral DTI, ximelagatran (**2**, Figure 1), a double prodrug converted in vivo to the active parent compound melagatran (**1**),[14] was approved for the treatment of VTE in Europe; however, it was withdrawn from the market in 2006 because of its hepatotoxicity.[15] The most recently approved DTI was dabigatran etexilate (**4**),[16] which is an orally available double prodrug of dabigatran (**3**) indicated for the prevention of VTE in patients undergoing total hip replacement and total knee replacement, as well as prevention of stroke in patients with atrial fibrillation.[17]

Both melagatran and dabigatran bear a highly basic benzamidine group that interacts with Asp189 in the S1 pocket. Several classes of DTIs employ an amidine group as P1 moiety, but despite their efficacy they suffer from poor oral bioavailability. As with dabigatran etexilate, the prodrug approach can be a solution to this problem. Nevertheless, the development of a new DTI lacking a highly basic P1 moiety, with good oral absorption, is still a challenge.

We previously described (iso)nipecotamide-based inhibitors of platelet aggregation induced by adenosine 5′-diphosphate (ADP).[18] Subsequently, some of them were suitably modified, providing compounds endowed with potential dual activity, that is, both inhibition of ADP-induced platelet aggregation and fXa inhibitory activities.[19] During the development of these compounds with dual function against thrombosis, the introduction of the highly polar amidine group on the piperidine nitrogen of the isonipecotamide derivative **5** (Figure 2), which is a moderate antiplatelet agent (IC_{50} = 68 μM) devoid of activity against the blood coagulation factors fIIa and fXa, yielded compound **6**, which exhibited some inhibition of the main blood coagulation factors with a preference for thrombin (K_i = 20.8 μM) while losing antiplatelet activity (IC_{50} = 768 μM).

As suggested by our early docking calculation performed with Glide,[20] compound **6** can bind into the catalytic site of bovine thrombin (PDB code 1UVT)[21] through the following three main interactions (Figure 3): (i) a salt bridge and a bifurcated hydrogen bonding between amidinium and carboxylate groups of Asp189 in the S1 pocket; (ii) H-bond of the amide NH to the backbone carbonyl group of Gly216 (S3); (iii) hydrophobic binding and CH···π interactions with Trp215 of the 4-F-phenyl group within the S4 site. The small hydrophobic S2 pocket appeared to be not involved in any interaction with the ligand.

In order to obtain new orally bioavailable fIIa/fXa inhibitors, we modified the structure of compound **6**, first exploring the effects of replacement of the P1 amidine group with less polar basic moieties on both the enzymes' inhibition potency and membrane permeability, as assessed by a parallel artificial membrane permeability assay (PAMPA),[22,23] and then trying to optimize physicochemical properties and positions of the substituents on the P4 phenyl group (Figure 2). The effects of

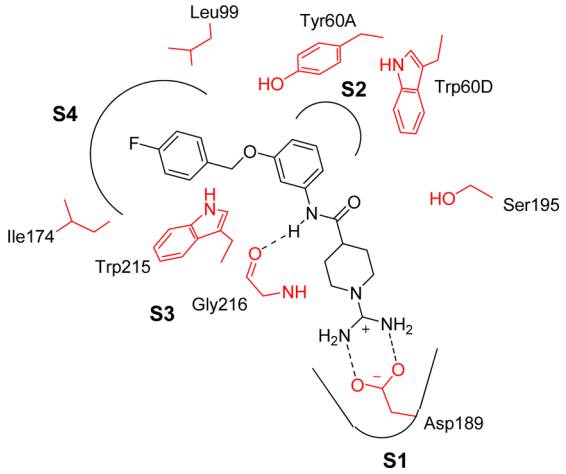

Figure 3. Schematic representation of the key interactions between compound **6** and thrombin, according to molecular modeling; key residues in the S1−S4 binding sites are shown in red.

some changes in the X-Y linker and amide group (*N*-methylation and reduction to amine) were also investigated.

In this work, we report the design and synthesis of *N*-[3-(benzyloxy)phenyl]isonipecotamide derivatives and analogues, most of them bearing the pyridin-4-yl group as the P1 moiety; their evaluation as inhibitors of fIIa, fXa, and other related serine proteases; and in vitro and ex vivo clotting assays. The structure−activity relationship (SAR) study is supported by molecular modeling and molecular dynamics (MD) results.

■ CHEMISTRY

The R^1-substituted 4-fluorobenzyloxyphenyl isonipecotamide derivatives were synthesized as shown in Schemes 1 (**7**−**9**) and 2 (**11**−**13a**, **15**).

Scheme 1. Synthetic Methods for Preparation of R^1-Bearing *N*-[3-(4-Fluorobenzyloxy)phenyl]piperidine-4-carboxamide Derivatives 7−9[a]

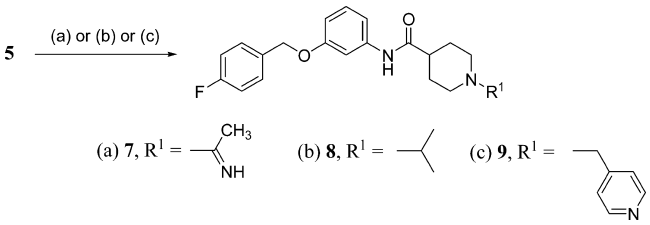

[a]Reagents and conditions: (a) $CH_3C(=NH)OC_2H_5 \cdot HCl$, TEA, EtOH, reflux, 6 h; (b) Me_2CO, $Na(CN)BH_3$, MeOH, rt, overnight; (c) 4-(bromomethyl)pyridine hydrobromide, K_2CO_3, dry DMF, rt, 48 h.

The acetamidine-bearing compound **7** was synthesized by refluxing the already reported compound **5**[19] with ethyl acetimidate hydrochloride in EtOH. The 1-isopropylpiperidine derivative **8** was synthesized by one-pot reductive alkylation, with acetone and $Na(CN)BH_4$. Compound **9** was synthesized in almost quantitative yield by reacting **5** with 4-bromomethylpyridine hydrobromide.

The preparation of 1-aza-heteroaryl-substituted piperidine-4-carboxamide derivatives **11**−**13a** and **15**, as shown in Scheme 2, proved to be more efficient than N^1-arylation of compound **5**. The 1-aza-heteroaryl-substituted isonipecotic acid intermediates (**10a**−**d**) were prepared starting from commercially available ethyl isonipecotate, which was refluxed in EtOH and K_2CO_3 with 2-chloropyrimidine (**10a**) or 2-bromopyridine (**10b**)[24] or 4-chloronitrobenzene (**10d**),[25] followed by hydrolysis of the ethyl esters with ethanolic NaOH. Compound **10c** was instead prepared in satisfactory yield by a one-pot reaction between ethyl isonipecotate, 4-chloropyridine hydrochloride, and triethylamine (TEA) in an EtOH/water mixture in a sealed tube.[26] The amide coupling between **10a**−**d** and 3-[(4-fluorobenzyl)oxy]aniline, with TBTU/DIPEA as the coupling reagents, finally produced compounds **11**, **12**, **13a**, and **14**. The 4-nitrophenyl derivative **14** was then reduced to the corresponding aminophenyl derivative **15** with hydrazine and Raney Ni.

The intermediate **10c** was further coupled with diverse 3-substituted aniline derivatives, producing *m*-benzyloxyphenyl 1-(pyridin-4-yl)isonipecotamides which differ in the physicochemical features and positions of R^4-substituents (Table 2), X-Y linker, and amide group modifications (Table 3). The aniline intermediates **I**−**IV** and **17** were synthesized through known methods as shown in Scheme 3.

The R^4-substituted 3-(benzyloxy)anilines of series **I** were prepared by benzylation of 3-nitrophenol, followed by reduction of the nitro group with hydrazine and Raney Ni in refluxing MeOH. The 3-F derivative was reacted with ethyl formate, followed by reduction with $LiAlH_4$, to give the secondary amine derivative **17** in high yield. The OH group of 3-nitrophenol was alkylated via a Mitsunobu reaction; subsequent hydrogenation over 10% Pd/C in EtOH provided the phenylethoxy derivatives **IIa** and **IIb**. The aniline intermediates **IIIa**,**b** were prepared by benzylation of 4(or 3)-fluorophenol with 1-(bromomethyl)-3-nitrobenzene, followed by reduction of the NO_2 group. The commercially available 3-nitrobenzaldehyde was converted to the aniline intermediates **IVa**,**b** by a Wittig reaction and subsequent catalytic hydrogenation.

The coupling between **10c** and the aniline intermediates **I**−**IV** was performed by use of TBTU/DIPEA as the coupling reagents in dry *N*,*N*-dimethylformamide (DMF) to prepare a number of *m*-benzyloxyphenyl 1-(pyridin-4-yl)piperidine-4-carboxamide derivatives bearing diverse R^4-substituents (**13**, **18**−**26**) and X-Y linkers (**32**−**34**), as shown in Scheme 4.

To verify the importance of the amide group, we investigated the effects of two simple modifications in **13b** (i.e., the most potent thrombin inhibitor of this series): (i) amide reduction (**29**) and (ii) NH methylation (**31**). Compound **29** was obtained in more than 90% yield by reduction of **13b** with BH_3−tetrahydrofuran (THF) complex. Unexpectedly, the coupling of **10c** with **17** produced **31** in very poor yield, which required laborious chromatographic purification. Compound **31** was then more efficiently synthesized by arylation with 4-chloropyridine of the amide intermediate **30**, which was obtained by coupling the Boc-protected isonipecotic acid and the *N*-methylaniline **17**, followed by the removal of the Boc group with HCl.

Experimental details on synthesis and analytical data for intermediates and final products can be found in the Experimental Section and Supporting Information.

While initial efforts to crystallize the most active compounds in complex with thrombin were unsuccessful, the crystal structure of the free ligand **13b**, as a representative example, was determined by X-ray diffraction. The structure of **13b** is shown in Figure 4 (crystal data and details on crystal packing are given in Supporting Information).

Scheme 2. Synthetic Methods for Preparation of N[1]-Aryl Derivatives of *N*-[3-(4-Fluorobenzyloxy)phenyl]piperidine-4-carboxamide, 11−15[a]

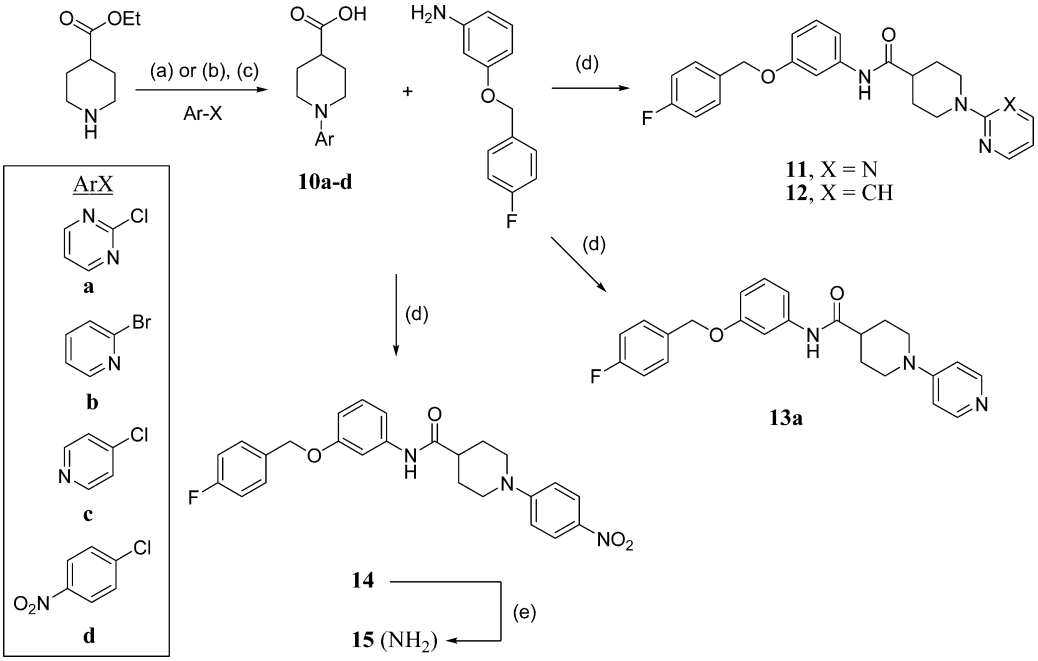

[a]Reagents and conditions: (a) absolute EtOH, K_2CO_3, reflux 4−40 h; (b) for **10c**, 4-chloropyridine hydrochloride, TEA, EtOH/water (1:3 v/v), sealed tube, 140 °C, 5 days; (c) NaOH, EtOH, reflux, overnight; (d) TBTU, DIPEA, dry DMF, rt, 72 h; (e) $N_2H_4{\cdot}H_2O$, Raney Ni, MeOH, reflux, 1 h.

Scheme 3. General Synthetic Methods for Preparation of 3-Substituted Aniline Intermediates I−IV and 17[a]

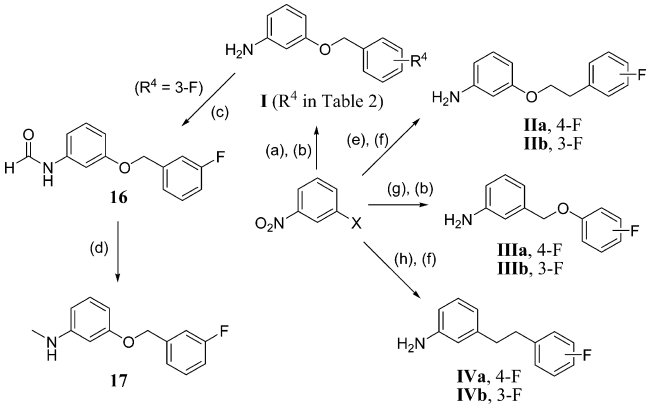

[a]Reagents and conditions: (a) X = OH, (R^4-substituted)benzyl bromide, K_2CO_3, dry DMF, rt, overnight; (b) $N_2H_4{\cdot}H_2O$, Raney Ni, MeOH, reflux, 1−4 h; (c) ethyl formate, reflux, 10 h; (d) $LiAlH_4$, dry THF, rt, overnight; (e) X = OH, 4(or 3)-(fluoro)phenethyl alcohol, PPh_3, DIAD, dry THF, rt, 48 h; (f) H_2, 10% Pd/C, EtOH, rt, 8 h; (g) X = CH_2Br, 4(or 3)-fluorophenol, K_2CO_3, dry DMF, rt, overnight; (h) X = CHO, 4(or 3)-(fluorobenzyl)triphenylphosphonium bromide, DBU, rt, 24 h.

RESULTS AND DISCUSSION

Inhibition constant (K_i) values for the newly synthesized compounds toward bovine fIIa and human fXa were measured via a chromogenic assay. The most active compounds were also tested for their inhibition potencies toward purified human fIIa and some related serine proteases, such as human recombinant fVIIa, human leukocyte elastase (LE), bovine trypsin (Try), and α-chymotrypsin (αCT). The K_i values are listed in Tables 1−3 and 6.

Replacement of the P1 Amidine Group with Less Polar Basic Moieties. We began by exploring the effects on fIIa/fXa inhibition potency and membrane permeability, as a main property affecting oral bioavailability, due to the replacement of the highly polar basic amidine group as P1 moiety in compound **6**. The enzymes' inhibition constants (K_i, micromolar), experimental ionization constants (pK_a), and permeability data (log P_e) are reported in Table 1.

Replacement of the amidine group in **6** with ethanimine (**7**), and even more with the isopropyl group (**8**), resulted in a decrease of inhibition potency, whereas among the 1-aza-heteroaryl-substituted compounds only the 1-pyridin-4-yl (**13a**) displayed a substantial (100-fold) increase in potency against fIIa (K_i = 0.211 μM) compared to **6** (K_i = 20.8 μM). The comparison between the inhibition data and pK_a values of the 1-aza-heteroaryl compounds supports the importance of the protonation degree and position of nitrogen within the aryl R^1 group. For the most potent inhibitor **13a**, only one pK_a value (8.9) was detected that corresponds to protonation of the pyridine nitrogen. Indeed, according to reported values and expert systems' calculations, the piperidine nitrogen is much less basic (ACDLabs calculated pK_a ca. −4.8), because of its aromatic conjugation with pyridin-4-yl group.[27] The same applies to compounds **11** and **12**. On the basis of the experimental pK_a, the pyridine nitrogen in **13a** should exist predominantly (ca. 89%) in protonated form at the assay pH (8.0) and be in a suitable position to form a salt bridge to Asp189 (S1), as shown by X-ray structures of thrombin in complex with other 4-pyridyl-containing fIIa inhibitors.[28,29] The 1-pyrid-2-yl isomer **12**, while having a basicity similar to that of **13a**, most likely loses potency because of the unsuitable

Scheme 4. Synthetic Methods for Preparation of Meta-Substituted *N*-Phenyl-1-(pyridin-4-yl)piperidine-4-carboxamide Derivatives 13 and 18−34[a]

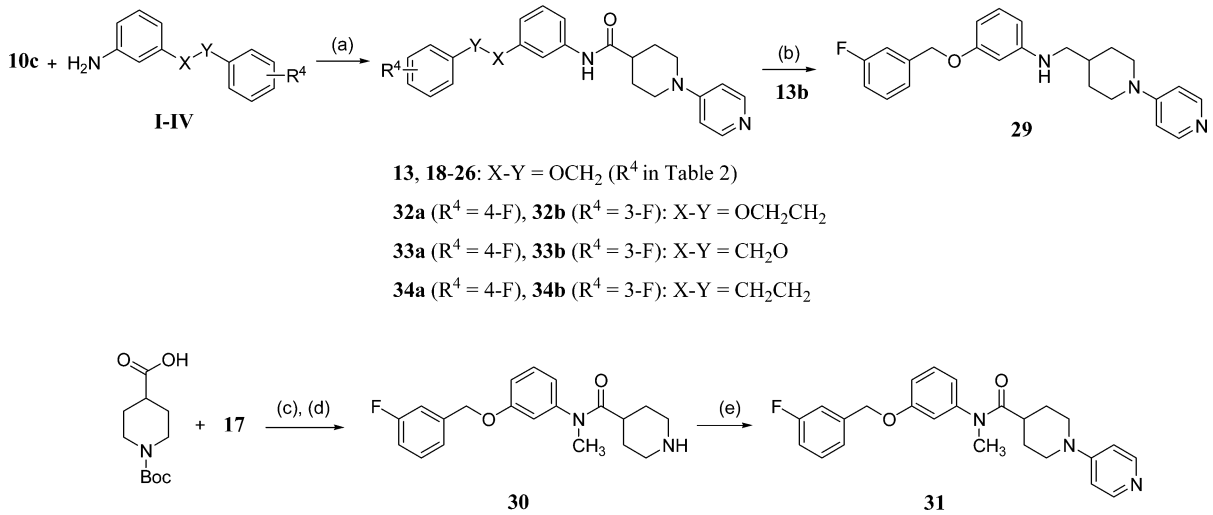

[a]Reagents and conditions: (a) TBTU, DIPEA, dry DMF, rt, 72 h; (b) BH_3-THF, rt, 24 h; (c) DCC, HOBt, dry THF, rt, 48 h; (d) HCl gas, $CHCl_3$; (e) 4-chloropyridine hydrochloride, absolute EtOH, TEA, reflux, 48 h.

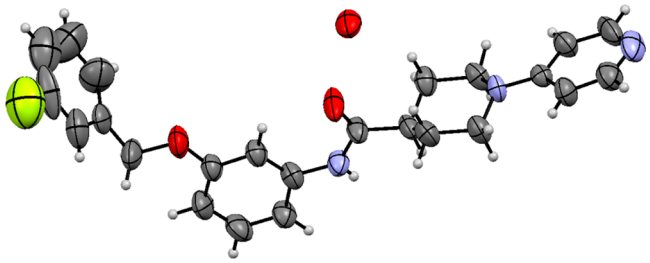

Figure 4. ORTEP drawing of **13b** crystal structure. C, O, N, H, and F atoms are shown in gray, red, light blue, white, and yellow, respectively. Ellipsoids represent the refined thermal factors. The O atom of methanol used as the crystallization solvent appears in the asymmetric unit of compound **13b**, whereas the C atom has not been unambiguously detected due to the poor electron density around the O atom. The **13b** crystal structure is stabilized by $\pi-\pi$ stacking intermolecular interactions between the 3-F-Ph moieties and between the pyridyl groups; also, a H-bond network between the N atom of pyridine, the amide CO and NH of two symmetry-related molecules, and the O atom of a MeOH molecule is involved in the formation of **13b** crystal packing.

location of pyridine nitrogen. Due to their lower basicity, and unfavorable nitrogen position as well, the 1-pyrimidin-2-yl (**11**) and 1-pyridin-4-ylmethyl (**9**) derivatives are orders of magnitude less potent than **13a**. The same arguments can be used for explaining the lower potency of **15**. Overall, even though there is no direct relationship with anti-fIIa activity, the ionization state proved to be important in enhancing the binding affinity to the active site's S1 pocket, as the data for the 1-aza-heteroaryl-substituted compounds showed (Table 1).

The effective permeability (P_e) of the majority of R^1-substituted isonipecotanilide-based fIIa inhibitors was measured by a hexadecane membrane (HDM) PAMPA. The HDM-PAMPA P_e values, which were shown to correlate with gastrointestinal (GI) absorption in humans for a number of drugs,[30] were taken as estimates of the abilities of our fIIa/fXa inhibitors to passively cross the GI tract, and then to have potential oral bioavailability, at the early stage of our molecular optimization study.

The experimental effective permeability data at pH 6.8 are spread over a range of 2 log units. According to reported criteria,[31] compounds **13a** and **15** can be considered as highly permeable ($P_e > 1 \times 10^{-6}$ cm·s^{-1}), whereas **5** and **6** have low permeability ($0.1 \times 10^{-6} \leq P_e < 1 \times 10^{-6}$ cm·s^{-1}). Two compounds, namely **9** and **11**, showed no permeability, most likely due to their slower diffusion through the unstirred water layer at the HDM/water interface. As a matter of fact, the amounts of **9** and **11** in the acceptor compartment were below the limits of the quantification via UV spectrophotometry and P_e could not be determined. In line with expectations, the permeability of **13a**, and of the weaker fIIa/fXa inhibitors **5** and **6** as well, slightly increased with decreasing acidity (log P_e values at pH 8; Table 1), whereas the less basic compounds **9** and **11** remained not permeable and **15** precipitated at the HDM/water interface. Reported permeability−pH profiles showed that the apparent pK_a of weak organic bases in HDM-PAMPA can be shifted toward lower pH.[30] However, the limited property space examined does not allow us to fully understand the relationships between structure and membrane permeation of the investigated compounds. We can just highlight that, for the permeable compounds at pH 6.8, the permeability increases as a function of the solvent-accessible surface area (SASA) descriptor calculated in silico on the ligand conformers in the top-ranked poses found by docking calculations (see below), using a probe with 1.4 Å^2 radius, by the module QikProp v 3.4 in Schrodinger Suite 2011. Indeed, the compounds with medium permeability, **5** (log P_e = −6.2) and **6** (log P_e = −6.0), have SASAs of 653 and 700 Å^2, respectively, whereas compounds **13a** (log P_e = −4.7) and **15** (log P_e = −4.0), showing high permeability, have SASAs of 756 and 780 Å^2, respectively. No clear relationship was observed with polar surface area (PSA) and other surface descriptors.

Compound **13a**, which combines the highest fIIa/fXa inhibition potency with the highest artificial membrane permeability, was chosen as starting point for further optimization of the P4 moiety.

Effects on fIIa/fXa Binding Affinities of R^4 Substituents at the Distal Phenyl Group. Starting from compound

Table 1. Effects of Replacement of the P1 Amidine Group on Thrombin and Factor Xa Inhibition Potency and Artificial Membrane Permeability (PAMPA)[a]

N.	R^1	FIIa K_i (μM)[a]	FXa K_i (μM)[a]	pK_a[b]	Log P_e[d] at pH 6.8	Log P_e[d] at pH 8.0
5	—H	>250	> 250	9.8	-6.2	-5.1
6		20.8	33.8	14.1[c]	-6.0	-5.8
7		> 250	57.3	12.7[c]		
8		> 250	> 250	9.4		
9		15.3	47.1	3.3, 6.5	n.p.	n.p.
11		26.8	91.6	6.0	n.p.	n.p.
12		> 250	78.0	8.5		
13a		0.211	1.10	8.9	-4.7	-4.4
15	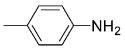	> 250	63.5	3.0, 6.0	-4.0	[e]

[a]Inhibition constants against bovine thrombin (fIIa) and human activated factor X (fXa) are means of three duplicate determinations (SEM < 5% of the mean). Compounds were tested at a maximum concentration of 250 μM. [b]Experimental pK_a values were determined by potentiometric titration (Sirius GLpKa). [c]Calculated pK_a values with ACD/Laboratories software (v. 12.0). [d]Log of the effective permeability coefficient, P_e ($cm \cdot s^{-1}$), as assessed by a parallel artificial membrane permeability assay (HDM-PAMPA) targeting gastrointestinal absorption (testosterone, log $P_e = -3.4$, was used as reference compound); np = not permeable. [e]Precipitation of solute at the hexadecane/water interface.

13a, we investigated the effects on fIIa/fXa inhibition potency of a number of R^4 substituents, which differ in electronic properties, lipophilicity, bulkiness, and hydrogen-bonding capacity, at the para, meta, and ortho positions of the P4 phenyl moiety (Table 2).

With only three exceptions (**18**, **20b**, and **21b**), all the R^4-substituted analogues showed fIIa selectivity. Importantly, the meta-F compound (**13b**), while improving selectivity toward fIIa over fXa by a factor of about 1000, showed K_i of 6 nM, with nearly 35-fold increase over the para-F isomer **13a** and 10-fold increase over the ortho-F isomer **13c**. Introduction of a second fluorine, such as in **13d** (2,4-F_2) and **13e** (3,5-F_2), did not increase the potency compared to monofluorinated compounds; only the 3,5-F_2 derivative **13e** maintained a potency close to that of 2-F congener **13c** but 10 times less active than the most potent compound **13b**. The replacement of F atom with Cl and Br, at either meta or para position, resulted in a lowering of the inhibition potency against fIIa (and fXa as well). With the monohalogenated compounds, it clearly appears that meta substitution (**13b**, **19b**, and **20b**), compared to para substitution (**13a**, **19a**, and **20a**), is more sensitive to the size of the halogen, given that the meta-fluorinated derivative **13b** displayed 26- and 3500-fold increase in potency over the bulkier 3-Cl (**19b**) and 3-Br (**20b**) compounds, respectively. Evidence of the role of F-bonding (i.e., fluorophilicity) in enhancing the binding affinity to thrombin and other related serine proteases of inhibitors bearing fluorinated aromatic moieties as P4 fragments has been already reported.[19,32,33] In the case of our inhibitors, once the most common protein−ligand interactions involving fluorinated P4 groups have been considered and the modeling results have been taken into account (see below), we believe that the highly polar C−F bond in meta position is suitably located for close contacts with the backbone carbonyls of amino acid residues inside the S4 pocket (e.g., Thr98, Glu97), thereby allowing the P4 moiety to establish therein C−F···C=O dipole−dipole interactions, which enhance the binding affinity and inhibitory potency.[32]

Besides the halogen substituents, we explored a number of other groups differing in electronic, lipophilic, steric, and H-bonding properties (Table 2). None of the substituents examined, at any position on the P4 phenyl group, showed inhibitory potency higher than that of the 3-F-Ph derivative

Table 2. Effect of R^4 Substituents on Binding Affinity to fIIa and fXa of *m*-Benzyloxyphenyl 1-(Pyridin-4-yl)piperidine-4-carboxamides

compd	R^4	K_i^a (μM) fIIa	fXa
18	H	39.5	7.46
13a	4-F	0.211	1.10
13b	3-F	0.006	5.64
13c	2-F	0.064	6.83
13d	2,4-F_2	4.64	8.80
13e	3,5-F_2	0.063	27.0
19a	4-Cl	0.260	29.6
19b	3-Cl	0.156	>250
20a	4-Br	2.03	37.1
20b	3-Br	20.9	6.31
21a	4-NO_2	5.85	6.00
21b	3-NO_2	26.8	6.73
22a	4-SO_2CH_3	0.124	7.73
22b	3-SO_2CH_3	15.9	15.6
22c	2-SO_2CH_3	12.3	35.1
23a	4-CF_3	3.40	48.5
24a	4-NH_2	10.0	25.0
24b	3-NH_2	13.3	36.1
25a	4-$CH_2N(CH_3)_2$	8.19	12.2
26a	4-OCH_3	2.03	11.1
26b	3-OCH_3	1.15	7.23
26c	2-OCH_3	1.30	16.4
26d	3,4-$(OCH_3)_2$	0.031	0.606
26e	3,5-$(OCH_3)_2$	0.083	126
26f	3,4-OCH_2O-	0.053	3.72

[a]Inhibition constants against bovine thrombin (fIIa) and human activated factor X (fXa) are means of three duplicate determinations (SEM < 5% of the mean). Compounds were tested at a maximum concentration of 250 μM.

13b. Moreover, no significant correlation (quantitative SAR) was found between pK_i values and lipophilicity, electronic, or steric parameters, alone or in linear/nonlinear combinations, suggesting that the R^4 substituents, irrespective of their electron-withdrawing/donating properties and/or hydrophilic/hydrophobic nature but in part depending on their bulkiness and/or H-bonding capacity, may induce conformational changes in the inhibitors, which then bind to the enzyme with different poses, more or less productive in terms of potency.

Among the investigated R^4 substituents, the electron-withdrawing and H-bond acceptor substituent SO_2CH_3 in the para position (**22a**) achieved nanomolar fIIa potency (124 nM) in the chromogenic assay. Notably, introducing two methoxy substituents on the P4 phenyl group with a 3,4-substitution pattern (**26d**) enhanced the potency with a K_i value in the low nanomolar range, however, with a marked decrease of selectivity over fXa. The almost equipotent 3,5-$(OCH_3)_2$ (**26e**) and 3,4-OCH_2O- (**26f**) analogues instead proved to be more selective than **26d** against fIIa. Actually, the piperonyl fragment had already successfully been employed to bind the thrombin S4 pocket, because it can strengthen binding by establishing a H-bond with the hydroxyl group of Tyr60A in the S2 subsite.[34]

The 3-F-benzyloxy ortho and para positional isomers (**27** and **28**, respectively) of the most active inhibitor **13b** were also tested (Figure 5). The ortho isomer **27** did not show significant inhibitory effects at the highest concentration tested (250 μM), and the para isomer **28** proved to be 3 orders of magnitude less potent than **13b** against both enzymes, which clearly showed that the meta-substituted isomer may be able to achieve a more correct orientation of the moieties interacting with the fIIa active site's pockets.

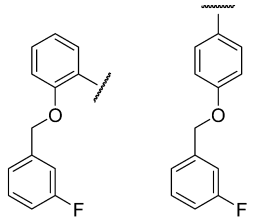

	27	**28**
FIIa, K_i	> 250 μM	6.70 μM
FXa, K_i	> 250 μM	25.1 μM

Figure 5. Enzymes' inhibition potency data of positional isomers at P4 3-fluorobenzyloxy moiety of compound **13b**.

Exploration of Modifications of the Amide Group and X-Y Linker. The removal of H-bond donor and acceptor in the central amide group of **13b**, through its reduction to amine (**29**) and N-methylation (**31**), led to a loss of activity toward fIIa but not fXa (which remained low), supporting the importance of H-bonds between the ligand and the backbone CO and/or NH of Gly216 in the S3 flat site (Table 3). To our surprise, the X-Y linker appeared as a key factor for fIIa inhibition potency, and OCH_2 proved to be, among those investigated in this study and a number of other more polar and rigid fragments (unpublished results), the linker that afforded the highest thrombin inhibition potency and selectivity. As a matter of fact, regardless of the position of F on the P4 phenyl group, either elongation (**32a,b**) or isosteric replacement (**33a,b** and **34a,b**) of the OCH_2 linker led to a loss in fIIa potency of at least 2 orders of magnitude, whereas in only two cases (**32a** and **33a**) was a substantial improvement of fXa inhibition potency observed.

Table 3. Effects of Modifications of the Amide Group and X-Y Linker on Binding Affinity to fIIa and fXa

compd	amide modification	X-Y linker	R^3	K_i^a (μM) fIIa	fXa
13b	CONH	OCH_2	3-F	0.006	5.64
29	CH_2NH	OCH_2	3-F	>250	3.83
31	$CON(CH_3)$	OCH_2	3-F	>250	23.6
32a	CONH	OCH_2CH_2	4-F	4.46	0.133
32b	CONH	OCH_2CH_2	3-F	0.488	2.14
33a	CONH	CH_2O	4-F	26.8	0.774
33b	CONH	CH_2O	3-F	18.2	>250
34a	CONH	CH_2CH_2	4-F	3.72	37.7
34b	CONH	CH_2CH_2	3-F	12.4	44.1

[a]Inhibition constants against bovine thrombin (fIIa) and human activated factor X (fXa) are means of three duplicate determinations (SEM < 5% of the mean). Compounds were tested at a maximum concentration of 250 μM.

We paid attention to variations in physicochemical properties (e.g., basicity, lipophilicity) possibly affecting the thrombin inhibition potency of the isosteric 3-F-Ph derivatives **13b**

(excellent inhibitor) and **33b** and **34b** (weak inhibitors), but the experimental measurements of pK_a (8.9, 8.8, and 8.7 for **13b**, **33b**, and **34b**, respectively) and 1-octanol/water log *D* at pH 7.4 (3.14, 3.02, and 3.58 for **13b**, **33b**, and **34b**, respectively) revealed no noteworthy variation in the ionization state and lipophilicity, which may be somehow related to the enzyme inhibition potency.

Binding Mode Evaluation by Molecular Modeling. To understand the presumable causes of the observed loss of affinity, we investigated the possible binding modes within the binding site of thrombin of the most active inhibitor **13b** compared with inactive compounds **29** and **31** and weak inhibitors **33b** and **34b**. The X-ray crystal structure of bovine thrombin in complex with the known 4-aminopyridine-based inhibitor BM14.1248 (PDB code 1UVT)[21] was retrieved from the RCSB Protein Data Bank and used in docking calculations with Glide software,[20] which had been proven to perform better than other automated docking programs with thrombin.[35] All flexible docking calculations were performed in the extra precision (XP) mode of Glide.[20c] The choice of the top-ranked pose for each ligand was made using the model energy score (Emodel), that combines Glide score, nonbonded interaction energy, and excess internal energy of the generated ligand conformation. As can be seen in Table 4, the Emodel score correlated reasonably well with the binding affinity, according to previous studies.[36,37] In our case, given the high similarity of the analyzed ligands, we were quite confident in using this scoring function to pick out the top-scored docking poses for visual inspection.

Table 4. Inhibition Constants and Calculated Interaction Energies of the Best Docked Ligand Structures on Thrombin

compd	pK_i	Emodel (kcal/mol)
13b	8.22	−86.46
29	<3.6	−73.37
31	<3.6	−69.30
33b	4.74	−75.01
34b	4.91	−79.21

As shown in Figure 6, the most potent inhibitor **13b**, in the top-ranked solution (panels A and C), binds to the enzyme pockets through three main interactions: (i) salt bridge, strengthened by a H-bond, between the pyridine NH^+ and the COO^- of Asp189, at the bottom of the enzyme S1 pocket; (ii) interaction of the meta-F-Ph group in the large hydrophobic S4 site; (iii) H-bond between the amide NH in **13b** and the Gly216 backbone CO (S3). No interaction with the small hydrophobic S2 pocket of the enzyme was revealed by the Glide search.

The N-methyl derivative **31** (Figure 6D) shows a complete reversal of the docking relative to the binding pose of **13b**: the P4 moiety (1-pyridin-4-ylpiperidine), which binds deep in the S1 pocket in the model of **13b**, occupies in part the S4 hydrophobic/aryl binding site, with the pyridinium group pointing out of the protein surface toward the solvent; the meta-F-Ph group interacts with the S1 pocket; and the H-bond between the amide group and Gly216 residue is lost. For compound **29**, Glide suggested two almost equally ranked docking poses, the first one resembling that of **13b** and the other being similar to that adopted by **31**.

According to the Glide solutions, compounds **33b** and **34b** adopt similar orientations but not overlapping conformations to that of **13b** (Figure 6B). They are closely superimposed in the molecular region encompassing the P4 pyridine and isonipecotamide moieties, with the amide NH forming a H-bond with Gly216, but they differ in folding of the P4 moiety, which is well accommodated for **13b** and fits poorly or not at all into the S4 hydrophobic pocket for **33b** and **34b**, respectively.

For **34b**, probably because of the greater flexibility of the CH_2CH_2 linker compared to OCH_2 (**13b**) and CH_2O (**33b**), the phenethyl P4 group appears more folded, positioned farther from the S4 site and pointed in the direction of the S2 pocket, without any clashing with Tyr60A and Trp60D. This S2 pocket is formed only in thrombin, whereas it is lacking in other related serine proteases, including fXa and the digestive enzymes chymotrypsin and trypsin.

On the basis of the Glide docking poses, it is reasonable to assume that the improvement in fIIa binding affinity of our compounds is related to the extent of the hydrophobic contact surface of the P4 side chain inside the S4 pocket and the H-bond between ligand NHCO and Gly216, as the anchoring binding of the P1 pyridine NH^+ and in the S1 pocket (Asp189) is a constant feature in both very active (**13b**) and weak inhibitors (**33b** and **34b**). Our computational models compare well enough with the data published a few years ago that showed for a series of fIIa inhibitors a mutual cooperative increase of hydrophobic interactions in the S4 pocket and H-bond involving Gly216, whose global strength is higher than that expected by simple additivity.[38] For instance, in that study Muley et al.[38] proved that an NH_2 group in the inhibitor that engage H-bond with the Gly216 backbone carbonyl oxygen may improve a close contact of the P4 moiety inside the S4 pocket by more than 59% (as assessed by the enhancement of binding affinity per square angstrom of hydrophobic contact surface in the S4 pocket) over inhibitors lacking this H-bond-donating group.

In order to further investigate how the CONH···Gly216 H-bond and P4−S4 hydrophobic contact in our three isosteric inhibitors **13b**, **33b**, and **34b** can interact with each other, molecular dynamics (MD) simulations were performed on the inhibitors (in their top-ranked docking poses) in complex with thrombin (details on MD procedure are given in the Experimental Section). An analysis of the MD trajectory over 2 ns was performed, and the average distances relative to key interactions engaging the inhibitors' groups and the protein residues/binding pockets are summarized in Table 5.

The MD simulation data along the trajectory suggest that the hydrogen-bonding salt bridge formed by the pyridinium NH^+ with the Asp189 COO^- in the S1 pocket is almost permanently maintained in all three inhibitors; the average distances between NH^+ and O1/O2 of the Asp189 COO^- oscillate just between 2.84 and 3.24 Å with standard deviations that in most cases do not significantly change. The H-bond NH···OC-Gly216 (S3) is maintained along the trajectory only for **13b**. In parallel, the time-averaged mean hydrophobic P4 side chain (3-F-Ph) distance to the S4 pocket is the shortest one (4.89 Å in **13b** versus 6.76 and 6.85 Å in **33b** and **34b**, respectively), with the lowest standard deviation. Overall, these MD simulation data seem to indicate that the shorter and stronger H-bond formed in **13b** by the amide NH with the Gly216 backbone CO most likely restricts the 3-F-benzyl movement inside the hydrophobic S4 binding site, thereby allowing this P4 side chain to spend more time in closer contacts (enhanced van der Waals interactions) with the S4 pocket surface.

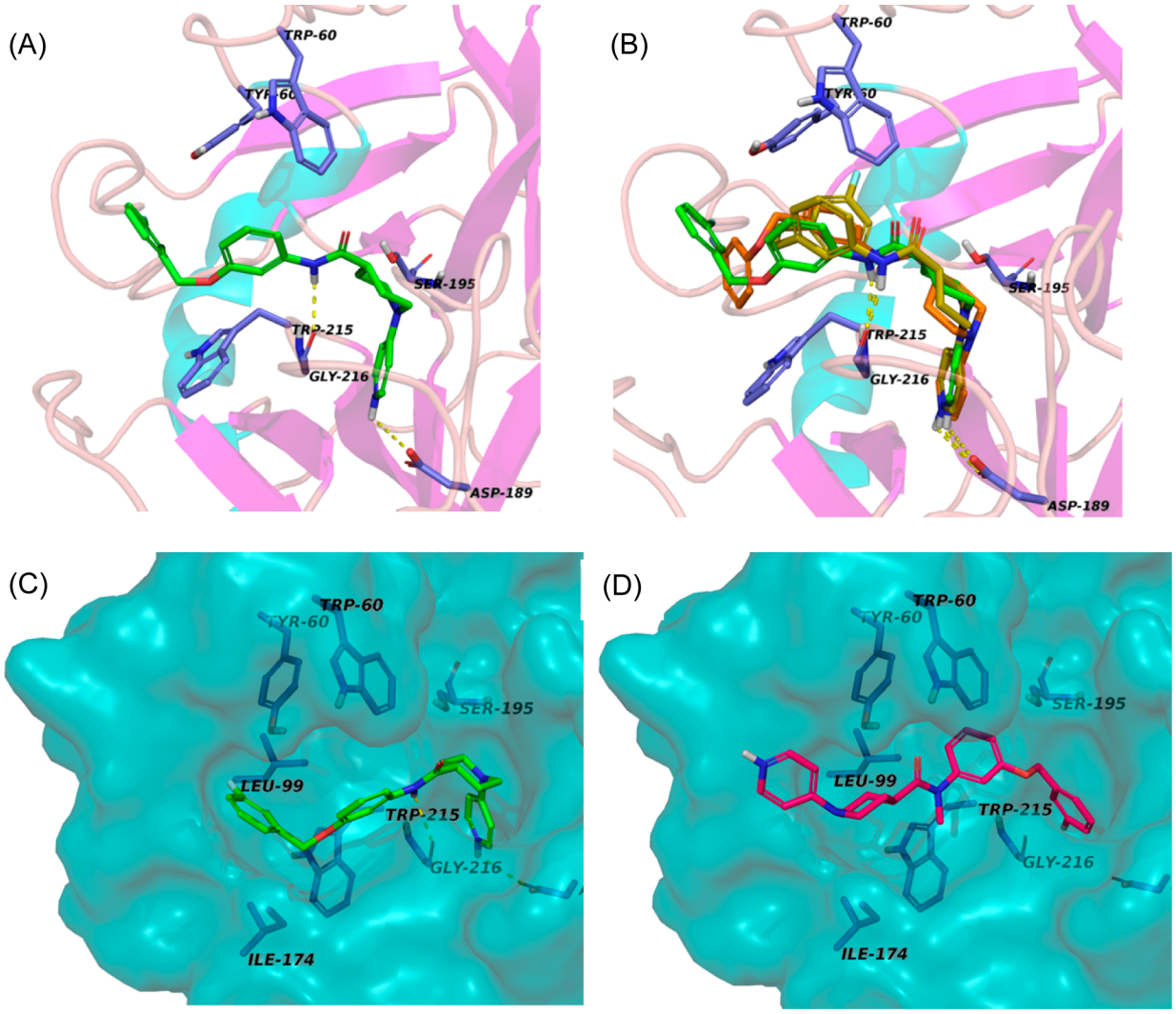

Figure 6. Glide top-ranked poses of 1-(pyridin-4-yl)piperidine-4-carboxamide-based inhibitors into the binding site of thrombin (PDB code 1UVT). The protein is shown in ribbon (panels A and B) or accessible surface representation (panels C and D), and the ligands and potentially interacting residues are shown in stick format (blue, nitrogen; red, oxygen; cyan, fluorine; carbon atoms, different colors; yellow dashed lines, H-bonds). (A) **13b** (green carbons); (B) overlay of **13b** (green carbons), **33b** (orange carbons), and **34b** (yellow carbons); (C) **13b** (green carbons); (D) **31** (purple carbons). The figures were drawn by PyMOL.

Table 5. Average Distances in Isosteric Inhibitors 13b, 33b, and 34b[a]

	time-averaged distance ± SD (Å)		
	13b	**33b**	**34b**
S1 Pocket: H-bond Pyridinium NH^+···Asp189			
NH^+···O1(O)C-Asp189	3.10 ± 0.31	2.98 ± 0.36	2.90 ± 0.37
NH^+···O2(O)C-Asp189	2.84 ± 0.26	2.94 ± 0.24	3.24 ± 0.54
S3 Pocket: H-bond CONH···Gly216			
CO···HN-Gly216	5.61 ± 1.10	4.29 ± 0.59	7.53 ± 1.65
NH···OC-Gly216	2.41 ± 1.00	6.41 ± 0.56	4.56 ± 0.89
S4 Pocket: 3-F-Ph Centroid−S4 Pocket Center[b]			
	4.89 ± 0.50	6.76 ± 1.23	6.85 ± 1.26

[a]Recorded over 2 ns along the MD trajectory. [b]Distance between the centroid of the P4 *m*-fluorophenyl group and the S4 pocket (calculated as the middle point between Leu99, Ile174, and Trp215 residues).

Selectivity over Other Serine Proteases and Anticoagulant Activity. The most potent fIIa inhibitor **13b** proved to be selective over a number of other serine proteases, with inhibition constants close to 7 μM for chymotrypsin, about 11 μM for human leukocyte elastase, and higher than 250 μM for trypsin (Table 6). It is roughly 1000-fold less potent on fXa and essentially inactive (K_i > 250 μM) on human recombinant fVIIa involved in the blood coagulation cascade. Other 1-pyridin-4-yl isonipecotamide derivatives chosen among the most potent fIIa inhibitors in the series were also assayed and found to be as selective as compound **13b**.

Compounds **13a** (R^4 = 4-F) and **13b** (R^4 = 3-F), which differ very much in affinity for bovine fIIa, were equipotent in inhibiting human wild-type thrombin. A striking difference in binding affinity to human and bovine fIIa was found not only for compound **13a**, which binds 15-fold better to human than to bovine fIIa, but also for the 3,4-$(OCH_3)_2$ derivative **26d**, that on the contrary binds 24-fold better to bovine than to human fIIa. These differences cannot be explained by Glide modeling calculations, which, when performed for investigating the docking of **13a**, **13b**, and **26d** to bovine fIIa (i.e., 1UVT) and two representative human fIIa structures (PDB codes 1JWT[39] and 2BDY[40]), provided almost similar binding modes and

Table 6. Inhibition Data against Blood Coagulation Factors and Other Serine Proteases, in Vitro Anticoagulant Activities, and Physicochemical Parameters of the Most Potent Thrombin Inhibitors Described in This Study

	K_i (μM)[a]							
	13a	**13b**	**13c**	**13e**	**22a**	**26d**	**26e**	**26f**
bfIIa	0.211	0.006	0.064	0.063	0.124	0.031	0.083	0.053
hfIIa	0.014	0.016	0.090	0.031		0.755		
hfXa	1.10	5.64	6.83	27.0	7.73	0.606	126	3.72
rfVIIa	>250	>250	>250	>250		>250		
bαCT	71.6	6.60	71.6	31.4	>250	71.5	33.8	>250
bTry	>250	>250	27.0	>250		27.0		
hLE	68.7	11.3	>250	>250		>250		
	Other Parameters							
	13a	**13b**	**13c**	**13e**	**22a**	**26d**	**26e**	**26f**
$aPTT_2$[b] (μM)	59.0	6.60	19.8	26.3	98.2	154	200	>200
pK_a[c]	8.9	9.0	9.2	9.2	9.1	9.2	8.9	9.1
log P^N[d]	5.1	5.0	4.9	5.2	4.9	4.9	4.9	4.9
log P_e[e]	−4.7	−4.8	−4.6	−5.0	−4.9	−4.5	−4.6	np

[a]Inhibition constants against bovine and human thrombin, human activated factor X, human recombinant activated fVII, bovine α-chymotrypsin and trypsin, and human leukocyte elastase are means of three duplicate determinations (SEM < 5% of the mean). Compounds were tested at a maximum concentration of 250 μM. [b]Concentrations of test compounds required to produce a doubling of the activated partial thromboplastin time (aPTT) of uninhibited clotting time in human plasma. The maximum concentration tested was 500 μM. [c]Experimental pK_a values determined by potentiometric titration (Sirius GLpKa). [d]1-Octanol/water partition coefficient of neutral form, as assessed by hydrophilic interaction liquid chromatography (HILIC; definitions and method details in Experimental Section). [e]Log of effective permeability coefficients, P_e (cm·s^{-1}) as assessed by a parallel artificial membrane permeability assay (PAMPA) targeting gastrointestinal absorption (testosterone, log P_e = −3.4, was used as reference compound); np = not permeable.

scores. On the other hand, the human thrombin 1JWT and 2BDY structures, compared to the bovine thrombin 1UVT, have more than 80% sequence identity and 100% identity in the inhibitors' binding sites (6 Å distance from the ligands' structures). It is likely that the observed differences in binding affinity can be ascribed to a different degree of purity of the enzymes used in the assays and thus probably to dissimilar interactions of the ligands with other components in the enzymes' samples.

Anticoagulant properties were assessed in vitro through the activated partial thromboplastin time (aPTT) clotting assay in pooled human plasma, and the anticoagulant potency was expressed as the concentration of inhibitor required to double the uninhibited clotting time ($aPTT_2$ in Table 6). Compound **13b** showed the best anticoagulant properties ($aPTT_2$ = 6.6 μM), whereas compound **13a**, albeit being an equipotent inhibitor on hfIIa, showed a significantly higher $aPTT_2$ value (59 μM). The differences in $aPTT_2$ values of the compounds in Table 6 are difficult to understand on the basis of either inherent fIIa/fXa inhibitory potencies or measured physicochemical properties. For example, compound **26f** (fIIa K_i = 53 nM) proved to be more than 10-fold less active in the aPTT clotting assay than **26d** (fIIa K_i = 31 nM), although they have similar thrombin inhibition potency, basicity, and lipophilicity. In early studies on potent noncovalent DTIs, it had been shown that the increase in plasma protein binding had detrimental effects on $aPTT_2$ values and antithrombotic activities of DTIs,[41] and more recently Remko,[42] on the basis of a detailed analysis of novel anticoagulant agents, concluded that compounds with high binding affinity to plasma components (e.g., proteins and phospholipids), albeit being potent fIIa/fXa inhibitors, generally show low effects on clotting time prolongation in plasma. In our case, the drop of activity in the aPTT assay, whose data were uncorrelated with the relative fIIa/fXa inhibition potency and/or lipophilicity, may indicate that the increase in binding affinity to plasma proteins and/or phospholipids of the examined compounds, notably those bearing methoxy and methylenedioxy substituents on the P4 phenyl ring, can cause a decrease in their anticoagulant activity.

The lipophilicity of the compounds in Table 6 was assessed by hydrophilic interaction liquid chromatography (HILIC), which is recognized to be suitable for accurate measurements of 1-octanol/water partition coefficients (log P^N) of the neutral form of basic compounds,[43] by a method already reported for similar compounds (details are given in the Experimental Section).[44] The log P values calculated from HILIC retention data demonstrate that these basic compounds are nearly isolipophilic in their neutral form (they span a range of just 0.3 log unit), whereas on the other hand suggest that lipophilicity has no significant effect either on their fIIa/fXa inhibition or on their anticoagulant potency.

The effective permeability coefficients (log P_e) as measured by PAMPA (Table 6) showed that, with the remarkable exception of the 3,4-OCH_2O- derivative (**26f**), which proved to be not permeable (a result that corresponds to the loss of activity in the aPTT clotting assay), all the most active antithrombin compounds cross the artificial membranes (log P_e values ranging from −4.5 to −5), with the most active fIIa inhibitor **13b** showing significant permeability (log P_e = −4.8). As all the permeable compounds show finite P_e values (including those reported in Table 1: log P^N = 3.7, 4.3, and 4.7 for compounds **5**, **6**, and **15**, respectively), with the exception of **15** (R^1 = 4-NH_2-Ph), there is a trend of linear correlation between log P_e and log P^N (n = 9, r^2 = 0.738; ρ = 1.1). In addition to PAMPA, the in vitro metabolic stability on microsomes remains to be investigated for a better druglikeness assessment of these anti-fIIa compounds.

Finally, for an early assessment of the oral anticoagulant effectiveness of compound **13b**, we examined its ex vivo activity after oral dosing in mice. Figure 7 shows that **13b**, administered via oral gavage at 100 mg·kg^{-1} dose, significantly prolonged plasma aPTT 1 h (28.9 ± 0.4 s) and 2 h (30.4 ± 3.3 s) after

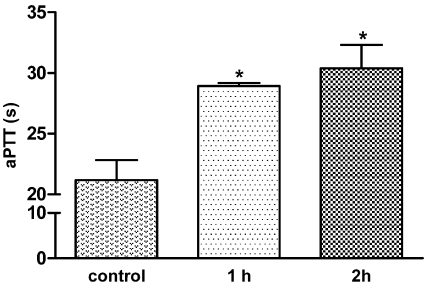

Figure 7. Ex vivo anticoagulant activity of compound **13b** (100 mg·kg^{-1}) after oral dosing in mice. Animals were administered via oral gavage with either vehicle (control) or test compound, and the activated partial thromboplastin time (aPTT) was measured 1 and 2 h after administration; aPTT values are expressed as means ± SEM of duplicate determinations in three mice per group (*P < 0.05 in Dunnett's test).

treatment versus controls (21.2 ± 4.9 s), both displaying significant clotting time prolongation (P < 0.05 in Dunnett's test). The mean percent aPTT prolongation was quantified as 36% and 43% at 1 and 2 h postadministration, respectively.

■ CONCLUSIONS

While many research groups, in both academia and industry, have attempted to develop new orally bioavailable DTIs, with wide therapeutic windows and fixed-dose administration, which could be safer and easier to use compared with warfarin, only the double prodrug dabigatran etexilate (**4**)[16] has been approved for prevention of stroke in patients with atrial fibrillation.[17c] In this study, we report new isonipecotamide-based compounds that are effective direct thrombin inhibitors (DTIs), showing in vitro and ex vivo anticoagulant activity in plasma. Starting from the simple *N*-[3-(4-fluorobenzyloxy)-phenyl]isonipecotamide bearing the amidine group at the piperidine N1 (**6**), that showed modest anti-fIIa and fXa potencies and poor membrane permeability (PAMPA), both enzymes' activities were significantly improved, with a net increase in the binding affinity toward fIIa. Structure−activity relationship studies, usefully complemented and supported by comparative molecular docking calculations and molecular dynamics simulations on some inhibitors in complex with thrombin, allowed us to expand the knowledge of the determinants for fIIa affinity and selectivity by N^1- and R^4-substituted-(benzyloxyphenyl)isonipecotamides, and led to identifying a number of new potent fIIa inhibitors with artificial membrane permeability (Table 6). Replacement of the 1-amidino group with 1-pyridin-4-yl group as the P1 moiety and, in particular, the displacement of fluorine from para to meta position of the P4 phenyl group, afforded compound **13b**, which showed excellent antithrombin activity (K_i = 6 nM) in the same range of dabigatran,[16] weak fXa inhibition (K_i = 5.64 μM), and remarkable selectivity versus a panel of serine proteases (>1000-fold lowest ratio). According to molecular modeling, **13b** closely fits in the fIIa active site's pockets S1, S3, and S4 (and not S2): the pyridinium group binds deep in the S1 pocket (Asp189), the amide NH forms a strong H-bond with the backbone CO of Gly216 in the flat S3 site, and the P4 3-F-Ph moiety binds to the hydrophobic S4 pocket. As expected by the PAMPA estimates and in vitro clotting assay in pooled human plasma, the most potent fIIa inhibitor **13b**, compared with controls, showed a 43% prolongation of clotting time in an ex vivo aPTT assay in mice at 2 h after oral dosing (100 mg·kg^{-1}). These data indicate that compound **13b**, in addition to being worthy of further pharmacological investigation, including a full ADMET characterization and in vivo antithrombotic profiling in comparison with the reference dabigatran etexilate, may be considered as a lead for further optimization of potent DTIs and fIIa/fXa dual inhibitors, as novel efficacious oral anticoagulant drugs safer than the existing ones.

■ EXPERIMENTAL SECTION

Chemistry. Melting points were determined by using the capillary method on a Stuart Scientific SMP3 electrothermal apparatus and are uncorrected. Elemental analyses (C, H, N) were performed on a Euro EA3000 analyzer (Eurovector, Milan, Italy) by the Analytical Laboratory Service of the Department of Pharmacy−Drug Sciences of the University of Bari (Italy), and the results agreed to within ±0.40% of theoretical values. Mass spectra were recorded on an Agilent gas chromatograph−mass spectrometer GC-MS 6890-5973. IR spectra were recorded via KBr disks on a Perkin-Elmer Spectrum One Fourier transform infrared spectrophotometer (Perkin-Elmer Ltd., Buckinghamshire, U.K.), and the most significant absorption bands are listed. ^{1}H NMR spectra were recorded at 300 MHz on a Varian Mercury 300 instrument. Chemical shifts are expressed in δ and the coupling constants J are in hertz (Hz). The following abbreviations are used: s, singlet; d, doublet; dd, doublet−doublet; t, triplet; m, multiplet. Signals due to NH and OH protons were located by deuterium exchange with D_2O.

Chromatographic separations were performed on silica gel 60 for column chromatography (Merck 70−230 mesh, or alternatively 15−40 mesh for flash chromatography). Unless otherwise stated, starting materials, and all chemicals and solvents as well, were purchased from Sigma−Aldrich. Several compounds were synthesized according to known procedures with slight modifications; their melting points and spectral data were in full agreement with those reported in literature, and no effort was made at this stage to optimize the yields.

1-Ethanimidoyl-*N*-{3-[(4-fluorobenzyl)oxy]phenyl}-piperidine-4-carboxamide Hydrochloride (7). To a solution of 365 mg (1 mmol) of **5**·HCl in 10 mL of absolute EtOH were added 741 mg (6 mmol) of ethyl acetimidate hydrochloride and 0.98 mL (7 mmol) of triethylamine, and the reaction mixture was refluxed for 6 h. After cooling and solvent removal, the residue was dissolved in 30 mL of EtOAc and the organic phase washed with 3 × 10 mL of brine, dried over Na_2SO_4, filtered, and concentrated. The crude oil was taken up in 10 mL of chloroform and treated with HCl gas. After solvent removal, 260 mg (64% yield) of **7** was obtained as a yellow oil. IR (film) 3415, 1670, 1606, 1223, 1154, 1934, 825, 775 cm^{-1}. ^{1}H NMR (300 MHz, DMSO-d_6) δ 10.18 (s, 1H), 9.30 (s, 1H), 8.73 (s, 1H), 7.56−7.37 (m, 3H), 7.27−7.07 (m, 4H), 6.67 (d, J = 7.0 Hz, 1H), 5.02 (s, 2H), 4.13 (d, J = 14 Hz, 1H), 3.92 (d, J = 14 Hz, 1H), (d, J = 12 Hz, 1H), 3.16 (d, J = 12 Hz, 1H), 2.73 (m, 1H), 2.28 (s, 3H), 1.92 (d, J = 10.5 Hz, 2H), 1.80−1.60 (m, 2H). ESIMS m/z 370 (MH$^+$). Anal. Calcd for $C_{21}H_{25}N_3O_2F$ × HCl: C, 57.07; H, 6.61; N, 9.51. Found: C, 57.32; H, 6.49; N, 9.33.

***N*-{3-[(4-Fluorobenzyl)oxy]phenyl}-1-isopropylpiperidine-4-carboxamide Hydrochloride (8).** To a solution of 300 mg (0.82 mmol) of **5**·HCl in 10 mL of MeOH and 5 mL of acetone was added portionwise 103 mg (1.64 mmol) of Na(CN)BH_3, and the reaction mixture was stirred at room temperature overnight. After solvent removal, the residue was dissolved in 50 mL of EtOAc and the organic phase was washed three times with 5% $NaHCO_3$ solution and brine, dried over Na_2SO_4, filtered, and concentrated. The crude oil was taken up in 10 mL of chloroform and treated with 5 mL of 1.25 M HCl solution in MeOH. After solvent removal, a solid residue was obtained, which was recrystallized from EtOAc/EtOH, and 110 mg (36% yield) of **8** was obtained as a brown solid, mp 145.3−148 °C. IR (KBr) 3223, 2944, 1646, 1606, 1226, 1154, 1012, 839, 776 cm^{-1}. ^{1}H NMR (300 MHz, $CDCl_3$) δ 7.47 (t, J = 1.0 Hz, 1H), 7.42−7.36 (m, 2H), 7.21 (br s, 1H), 7.20 (t, J = 8 Hz, 2H), 7.06 (t, J = 8.5 Hz, 2H), 6.91 (dd, J_1 = 8.0 Hz, J_2 = 1.5 Hz, 1H), 6.70 (dd, J_1 = 7.5 Hz, J_2 = 1.5 Hz, 1H), 5.02

(s, 2H), 2.99 (d, J = 12 Hz, 2H), 2.85 (heptet, J = 8.0 Hz, 1H), 2.35−2.15 (m, 2H), 2.05−1.95 (m, 2H), 1.07 (d, J = 8.0 Hz, 6H). ESIMS m/z 371 (MH^+). Anal. Calcd for $C_{22}H_{28}N_2O_2F \times HCl$: C, 64.94; H, 6.94; N, 6.88. Found: C, 65.12; H, 6.49; N, 6.93.

***N*-{3-[(4-Fluorobenzyl)oxy]phenyl}-1-(pyridin-4-ylmethyl)-piperidine-4-carboxamide (9).** To a solution of 200 mg (0.55 mmol) of **5**·HCl in 10 mL of DMF were added 149 mg (1.08 mmol) of K_2CO_3 and 91 mg (0.36 mmol) of 4-bromomethylpyridine hydrobromide, and the reaction mixture was stirred at room temperature for 48 h and then poured into ice−water. The resulting precipitate was collected, washed with Et_2O, and then filtered to provide the title compound as a pale brown solid (147 mg, 97% yield), mp 155−158 °C. IR (KBr) 3225, 1648, 1439, 1224, 1154, 1010 cm^{-1}. ^1H NMR (300 MHz, DMSO-d_6) δ 9.82 (s, 1H), 8.48 (d, J = 5.8 Hz, 2H), 7.49−7.46 (m, 2H), 7.44 (s, 1H), 7.31 (d, J = 5.8 Hz, 2H), 7.22−7.08 (m, 4H), 6.65 (d, J = 9.0 Hz, 1H), 5.01 (s, 2H), 3.48 (s, 2H), 2.83−2.80 (m, 2H), 2.33−2.25 (m, 1H), 1.99 (d, J = 9.0 Hz, 1H), 1.95 (d, J = 8.5 Hz, 1H), 1.74−1.62 (m, 4H). ESIMS m/z 420 (MH^+). Anal. Calcd for $C_{25}H_{26}N_3O_2F$: C, 71.58; H, 6.25; N, 10.02. Found: C, 71.25; H, 6.49; N, 9.93.

General Procedure for Synthesis of Substituted *N*-[(Benzyloxy)phenyl]-1-arylpiperidine-carboxamide Derivatives (11−13, 18−29, and 31−34). Yields and spectroscopic data of compounds that have been prepared following the same route are reported in Supporting Information. The synthesis of *N*-{3-[(4-fluorobenzyl)oxy]phenyl}-1-pyridin-2-ylpiperidine-4-carboxamide **13a** is reported here as an example.

To a solution of 500 mg (2.42 mmol) of 1-(pyridin-2-yl)piperidine-4-carboxylic acid **10c** in 10 mL of dry DMF were added 777 mg (2.42 mmol) of TBTU, 1.686 mL (9.68 mmol) of DIPEA, and, after 30 min, 475 mg (2.91 mmol) of 3-[(4-fluorobenzyl)oxy]aniline.[19] The reaction mixture was stirred at room temperature for 72 h and then poured on ice. The resulting precipitate was filtered, collected, and washed with Et_2O to yield the title compound (when necessary, the crude products were recrystallized from acetone and MeOH) as a pale brown solid, 100 mg (45% yield), mp 144−146 °C. IR (KBr) 3232, 1649, 1596, 1489, 1439, 1226, 1207, 1154, 1011 cm^{-1}. ^1H NMR (300 MHz, DMSO-d_6) δ 9.89 (s, 1H), 8.08 (d, J = 3 Hz, 1H), 7.51−7.39 (m, 4H), 7.22−7.12 (m, 4H), 6.82 (d, J = 8.5 Hz, 1H), 6.65 (d, J = 7.0 Hz, 1H), 6.60−6.56 (m, 1H), 5.01 (s, 2H), 4.33 (d, J = 13 Hz, 2H), 2.83 (d, J = 12 Hz, 1H), 2.79 (d, J = 12 Hz, 1H), 2.61−2.53 (m, 1H), 1.82−1.78 (m, 2H), 1.63−1.52 (m, 2H). ESIMS m/z 406 (MH^+). Anal. Calcd for $C_{24}H_{24}N_3O_2F$: C, 71.09; H, 5.97; N, 10.36. Found: C, 71.12; H, 6.29; N, 10.25.

1-(4-Aminophenyl)-*N*-{3-[(4-fluorobenzyl)oxy]phenyl}-piperidine-4-carboxamide (15). To a solution of 100 mg (0.22 mmol) of **14** (its synthesis is described in the Supporting Information) in 20 mL of MeOH were added 0.1 mL of hydrazine hydrate and 0.1 mL of activated Raney Ni suspension. The reaction mixture was refluxed for 0.5 h until disappearance (as monitored by thin-layer chromatography, TLC) of the starting material and then cooled and filtered through a Celite pad. The filtrate was concentrated under reduced pressure to provide 60 mg (65% yield) of **15** as a brown solid, mp 159−161 °C. IR (KBr) 3435, 1671, 1261, 1153, 1022, 800 cm^{-1}. ^1H NMR (300 MHz, acetone-d_6) δ 9.12 (br s, 1H), 7.60 (s, 1H), 7.54 (dd, J_1 = 5.5 Hz, J_2 = 3.0 Hz, 2H), 7.20−7.13 (m, 4H), 6.76 (d, J = 9.0 Hz, 2H), 6.72−6.68 (m, 1H), 6.59 (d, J = 9.0 Hz, 2H), 5.08 (s, 2H), 3.48−3.43 (m, 2H), 2.81 (br s, 2H), 2.61−2.51 (m, 2H), 2.47−2.36 (m, 1H), 1.95−1.90 (m, 4H). ESIMS m/z 420 (MH^+). Anal. Calcd for $C_{25}H_{26}N_3O_2F \times H_2O$: C, 68.63; H, 6.45; N, 9.60. Found: C, 68.80; H, 6.49; N, 9.73.

3-(3-Fluorobenzyloxy)-*N*-methylbenzenamine (17). A solution containing 1.29 g (5.96 mmol) of 3-[(4-fluorobenzyl)oxy]aniline in 10 mL of ethyl formate was refluxed for 20 h. The mixture was cooled to room temperature and concentrated under reduced pressure to provide 1.43 g (98% yield) of *N*-[3-(3-fluorobenzyloxy)phenyl]-formamide **16**. Then 1.88 g (7.67 mmol) of the crude product **16** was dissolved in 10 mL of dry THF and added dropwise to a cooled suspension of 0.436 g (11.50 mmol) of $LiAlH_4$ in 30 mL of dry THF. The reaction mixture was stirred for 1 h at 0 °C and then for 20 h at room temperature. After cooling to 0 °C, the reaction was quenched by addition of 10 mL of saturated Na_2SO_4 solution, filtered, and washed with Et_2O. The organic phase was dried over Na_2SO_4, filtered, and concentrated under reduced pressure to yield 1.57 g (84% yield) of 3-(3-fluorobenzyloxy)-*N*-methylbenzenamine **17** as an oil. IR (film) 3414, 1618, 1592, 1514, 1497, 1448, 1261, 1194, 1166, 1037, 932, 868, 828, 774, 686 cm^{-1}. ^1H NMR (300 MHz, $CDCl_3$) δ 7.37−7.27 (m, 1H), 7.25−7.14 (m, 2H), 7.09 (t, J = 8.0 Hz, 1H), 7.00 (t, J = 8.2 Hz, 1H), 6.34−6.23 (m, 3H), 5.03 (s, 2H), 3.77 (br s, 1H), 2.82 (s, 3H).

***N*-{3-[(3-Fluorophenoxy)methyl]phenyl}-*N*-[(1-pyridin-4-yl-piperidin-4-yl)methyl]amine (29).** To a 0 °C cooled solution of 1.566 g (3.86 mmol) of compound **13b** in 20 mL of THF was added 27 mL of a solution of 1 M borane−THF complex, and the reaction mixture was stirred at room temperature for 24 h. After quenching by addition of 6 N HCl (20 mL), water (20 mL), and MeOH (40 mL), stirring was prolonged for 24 h. The resulting solution was then concentrated under reduced pressure and the aqueous solution was basified to pH 12 with 4 N NaOH and extracted three times with EtOAc (20 mL). The combined organic layers were dried, filtered, and concentrated under reduced pressure to provide 1.42 g of **29** (94% yield) as a brown solid, mp 159−161 °C. IR (KBr) 3246, 1616, 1600, 1543, 1513, 1194, 1054, 990, 804, 771, 752, 699 cm^{-1}. ^1H NMR (300 MHz, DMSO-d_6) δ 8.09 (d, J = 5.0 Hz, 2H), 7.44−7.37 (m, 1H), 7.25−7.20 (m, 2H), 7.12 (t, J = 9.0 Hz, 1H), 6.92 (t, J = 8.5 Hz, 1H), 6.78 (d, J = 5.0 Hz, 2H), 6.18−6.12 (m, 3H), 5.69 (t, J = 6.0 Hz, 1H), 5.02 (s, 2H), 3.91 (d, J = 13 Hz, 2H), 2.87 (t, J = 6.0 Hz, 2H), 2.78 (d, J = 13 Hz, 1H), 2.74 (m, J = 13 Hz, 1H), 1.78 (d, J = 11 Hz, 2H), 1.44−1.39 (m, 1H), 1.21−1.09 (m, 2H). ESIMS m/z 420 (MH^+). Anal. Calcd for $C_{24}H_{26}N_3OF$: C, 73.63; H, 6.69; N, 10.73. Found: C, 73.51; H, 6.75; N, 10.93.

***N*-[3-(3-Fluorobenzyloxy)phenyl]-*N*-methylpiperidine-4-carboxamide (30).** To a solution of 1.71 g (7.48 mmol) of 1-(*tert*-butoxycarbonyl)piperidine-4-carboxylic acid[19] in 25 mL of THF were added 0.92 g (6.80 mmol) of 1-hydroxybenzotriazole hydrate (HOBt), 1.403 g (6.80 mmol) of *N*,*N*′-dicyclohexylcarbodiimide (DCC), and, after 30 min, 1.57 g (6.80 mmol) of 3-(3-fluorobenzyloxy)-*N*-methylbenzenamine **17**, dissolved in 5 mL of dry THF. The reaction mixture was stirred for 48 h at room temperature, and then DCU was filtered off and the filtrate was concentrated to dryness. The oil residue was dissolved in 100 mL of EtOAc, and the organic phase was washed sequentially with 3 × 20 mL of saturated $NaHCO_3$, 1 N HCl, and brine, dried, filtered, and concentrated under reduced pressure. The obtained oil residue was chromatographed on silica gel (mobile phase EtOAc/40−60 petroleum ether, 3:7 v/v), to provide the N-Boc-protected derivative. After removal of the Boc protecting group, by bubbling HCl gas through a cooled $CHCl_3$ solution, the obtained HCl salt was poured into water and the solution was brought to pH 12 by adding 4 N NaOH. The aqueous basic suspension was extracted three times with EtOAc, and the combined organic layers were dried, filtered, and concentrated to provide 1.22 g (52% yield) of **30**, as a brown oil. ^1H NMR (300 MHz, $CDCl_3$) δ 7.39−7.27 (m, 2H), 7.20−7.13 (m, 2H), 7.05−6.91 (m, 2H), 6.80−6.74 (m, 2H), 5.09 (s, 2H), 3.22 (s, 3H), 2.99 (d, J = 13 Hz, 2H), 2.36−2.25 (m, 3H), 1.73−1.62 (m, 3H), 1.52−1.48 (m, 2H).

***N*-{3-[(3-Fluorophenoxy)methyl]phenyl}-*N*-methyl-1-pyridin-4-ylpiperidine-4-carboxamide (31).** A mixture, containing 366 mg (1.07 mmol) of **30**, 161 mg (1.07 mmol) of 4-chloropyridine hydrochloride,and 0.45 mL (3.21 mmol) of TEA in 4 mL of absolute EtOH, was stirred for 2 days at 140 °C in a sealed tube. After cooling to room temperature, the mixture was concentrated under reduced pressure and the oil residue was dissolved in 30 mL of EtOAc and washed twice with 20 mL of 2 N NaOH. The organic phase was dried, filtered, and concentrated under reduced pressure to provide 373 mg of **31** (83% yield), as a dark brown oil. IR (liquid) 1652, 1592, 1226, 1028, 989, 873, 784 cm^{-1}. ^1H NMR (300 MHz, DMSO-d_6) δ 8.09 (d, J = 6.0 Hz, 2H), 7.47−7.25 (m, 4H), 7.18−7.11 (m, 1H), 7.04−6.85 (m, 3H), 6.72 (d, J = 6.0 Hz, 2H), 5.17 (s, 2H), 3.80 (d, J = 13 Hz, 2H), 3.31 (s, 3H), 2.73−2.78 (m, 1H), 2.42−2.54 (m, 1H), 1.96−2.06 (m, 1H), 1.64−1.34 (m, 4H). ESIMS m/z 420 (MH^+). Anal. Calcd for

$C_{25}H_{26}N_3O_2F \times H_2O$: C, 68.63; H, 6.45; N, 9.60. Found: C, 68.72; H, 6.59; N, 9.83.

X-ray Crystal Structure Analysis of 13b. Crystals of **13b** suitable for X-ray structure determination were obtained by slowly adding dichloromethane to a methanolic solution of the compound. The crystal structure was determined from X-ray single-crystal diffraction data. The crystal of **13b** was mounted on a glass fiber and diffraction measurements were carried out on a Bruker-Nonius Kappa charge-coupled device (CCD) diffractometer equipped with a CCD area detector, a Mo fine focus X-ray tube (λ = 0.710 73 Å), and a 0.35 mm capillary optical collimator to improve radiation intensity and reduce beam divergence. Crystallographic parameters and data collection information are reported in Supporting Information (Tables S1 and S2).

The structure was solved by direct methods with SIR2011[45] and refined by full matrix least-squares on F^2 with SHELXL-97.[46] Friedel pairs were merged before the final refinement. The positions of the H atoms bonded to N atoms were obtained from the difference Fourier map and were refined. The remaining H atoms were placed in geometrically calculated positions and were refined by use of a riding model, with C−H = 0.96 and 0.93 Å for $C_{sp^3}H$ and $C_{ar}H$, respectively. The thermal factors of non-H atoms were refined anisotropically, while those of H atoms were considered isotropic and linked to the equivalent isotropic thermal factors of the carrier non-H atom: U_{iso} (H) = $1.2U_{eq}$ (non-H). The refined structure of **13b**, with ellipsoids representing the refined thermal factors, generated with ORTEP-3,[47] is shown in Figure 4. The refinement parameters (Table S3) and details on crystal packing are reported in Supporting Information.

Potentiometric Determination of Ionization Constants. Experimental ionization constants (pK_a) were determined by potentiometric titration on a Sirius GLpKa instrument, and data were treated by RefinementPro software (Sirius Analitical Ltd., Forest Row, East Sussex, U.K.). An appropriate amount of each compound was dissolved in 20 mL of ionic strength adjusted water (0.15 M KCl solution) to achieve a final sample concentration around 5×10^{-4} M. All the titrations were recorded in the pH range between 1.8 and 12.2 at 25 ± 0.5 °C, with standardized 0.5 M HCl and 0.5 M carbonate-free KOH as titrating agents. Experiments were carried out under a slow nitrogen flow to avoid CO_2 absorption under high-pH conditions.[48] All the measurements were carried out in triplicate, and precise pK_a values were calculated from the Bjerrum differential curve as the pH value required to have 50% of dissociated form of test compound. For compounds with low aqueous solubility, methanol, ranging from 20% to 60% (v/v), was added as the cosolvent and the aqueous pK_a was then extrapolated by use of the Yasuda−Shedlovsky equation.

Determination of Lipophilicity Parameters by Hydrophilic Interaction Liquid Chromatography. Retention measurements were performed at 23 °C and a flow rate of 1.0 mL·min^{-1} by using as the stationary phase a ZIC-pHILIC column (sulfoalkylbetaine phase on a polymeric support, 10 cm × 4.6 mm, 5 μm) from SeQuant (Umeå, Sweden). All the experiments were performed on a Merck Hitachi EliteLaChrom liquid chromatograph (Merck, Darmstadt, Germany, and Hitachi Instruments, Inc., San Jose, CA) equipped with L-2200 auto sampler, L-2130 pump, L-7614 degasser, and L-2400 UV detector, operating at 254 nm for all compounds. The chromatographic system was controlled by a EzChrom Elite System Manager software version 3.1.7 (Merck Hitachi). Phoebus software 1.0 (Sedere, Centre Analyze, Orleans, France) was used to prepare buffer (trifluoroacetic acid/ammonium) at pH 2 and ionic strength (I) equal to 100 mM.

According to Bard et al.,[43] the difference parameter ($\Delta\log k_{0-95}$) between two isocratic log k values of the basic compounds in their cationic forms—namely, log k_0, which is the log k obtained in 100% aqueous buffer (pH 2) mobile phase, and log k_{95}, which is the isocratic log k measured in 95% (v/v) acetonitrile−aqueous buffer (pH 2) mobile phase—allows the partition coefficient of their neutral form (log P^N) to be calculated for basic compounds through the following validated correlation equation:[43] $\log P^N = 1.07\ \Delta\log k_{0-95} + 0.61$.

Permeability Measurements. Parallel artificial membrane permeability assay (PAMPA) was used to determine effective permeability coefficients P_e (centimeters per second), in a 96-well microtiter filter plates, on polycarbonate filter of 3 μm pore size, 10 μm thickness, and 5−20% porosity (Millipore AG, Volketswil, Switzerland), according to the procedure of Wohnsland and Faller,[30] and testosterone (log P_e = −3.4) was used as the reference compound.[49]

Each compound, dissolved in DMSO (concentration range 10^{-2}−10^{-3} M, according to solubility and UV detection limits), was tested at least in triplicate at pH 6.8 (and pH 8.0 as well) in iso-pH conditions (i.e., the same pH in donor and acceptor compartments). Each well was coated with 15 μL of hexadecane (5% in hexane solution) for at least 20 min to completely evaporate the hexane, whereas the Teflon acceptor plate was hydrated with 280 μL of pH 6.8 phosphate buffer containing 5% DMSO. The donor plate was placed upon and filled with 280 μL of pH 6.8 phosphate buffer containing 5% DMSO test compound solution, and the resulting chamber was incubated at room temperature under constant shaking (150 rpm) for 5 h, when it was carefully disassembled and both acceptor and donor compartment solutions were transferred into UV-quartz plates and absorptions were measured (PowerWave, Bio-Tek Instruments, Inc.) at the compound's λ_{max}. Hexadecane membrane stability was tested at the end of incubation time by electrical resistance measurements, by use of an electrometer system for PAMPA assays (EVOMX and MULTI96, World Precision Instruments, Sarasota, FL). The effective permeability P_e was determined from the ratio $C_A(t)/C_D(t_0)$ between UV absorbances in the acceptor compartment at time t and in the donor well at time t_0. The permeability equation used includes a term related to membrane compartment:[50]

$$P_e = -\frac{2.303V_D}{A(t-\tau_{lag})}\left(\frac{V_A}{V_A+V_D}\right)\log\left[1-\left(\frac{V_A+V_D}{V_D(1-R)}\right)\frac{C_A(t)}{C_D(t_0)}\right]$$

where A is the accessible filter area (0.24 cm^2) multiplied by nominal porosity of 13% according to manufacturer, t is the incubation time (seconds), V_A and V_D are the volumes (cubic centimeters) in the acceptor and donor wells, R is the retention factor, defined as the mole fraction of compound lost in the membrane and in microplates (i.e., filters and plate materials), and τ_{lag} is the steady-state time (seconds), which is the time needed for the permeant's concentration gradient to become stabilized; because in PAMPA experiments τ_{lag} for saturation of the membrane is very shorter than the total permeation time, it is usually neglected.[51] The retention factor R is defined as

$$R = 1 - \frac{C_D(t)}{C_D(t_0)} - \frac{V_A}{V_D}\frac{C_A(t)}{C_D(t_0)}$$

Since permeation can be attributed to the neutral species alone, particularly for compounds with un-ionized fraction $f_{ui} > 0.1$, the effective permeability coefficient P_e is divided by the un-ionized fraction f_{ui}, calculated for compounds with a single acidic or basic group according to the dissociation constant (pK_a) and the pH in each compartment, as follows:

$$f_{ui} = \frac{1}{1+10^g}$$

where $g = (\mathrm{pH} - pK_a)$ for acids and $g = (pK_a - \mathrm{pH})$ for bases.

Molecular Modeling. All calculations were performed with programs included in the Schrodinger Suite 2011.[56] The X-ray crystal structure of bovine thrombin in complex with the 4-aminopyridine-based inhibitor BM14.1248 (PDB code 1UVT)[21] was retrieved and used as the target in docking calculations. After being prepared with the standard options of the Protein Preparation Wizard protocol, the docking grid was calculated by placing the coordinates of the center of mass of the cocrystallized ligand as the center of a cubic box, having a side length of 20 Å. All the possible protonation states at pH 7.0 ± 2 were assigned to the inhibitor molecules by use of the LigPrep module version 2.5 (default options). All docking calculations were performed in the extra precision (XP) mode of Glide version 5.7,[20] and either GlideScore scoring function or the composite Emodel score were used to rank the poses of each ligand. The Emodel scoring function was

finally preferred to select the top-ranked poses to be visualized, due to its better correlation with the experimental affinity data. The surface area descriptors (SASA, PSA, etc.) of each ligand in the top-ranked pose were calculated by use of the QikProp 3.4 module available in Schrodinger Suite 2011.

Molecular Dynamics Simulations. Complexes between the protein and the ligands **13b**, **33b**, and **34b**, in the top-ranked poses as identified according the Emodel scoring function, were stored and used for MD simulations, performed with the Desmond package version 3.0.[52] The protein−ligand complexes were first solvated with TIP3P water molecules, 0.15 M NaCl, and neutralized with proper counterions by use of the System Builder module of Desmond. A triclinic box, with each side at a minimum distance of 10 Å from any atom of the complex, was used. For the ligands the OPLS 2005 force field in a canonical ensemble (NVT) was used; all the remaining default settings have been left. The dynamic protocol was set in subsequent steps: (i) a relaxing minimization, followed by (ii) a progressive increase of temperature to 300 K in 140 ps, and finally (iii) a production run of 2 ns. Frames of the simulation were recorded every 5 ps. The 2 ns trajectories were analyzed by use of the simulation event analysis tool, as implemented in the Desmond package, whereas VMD[53] was used for visualization purposes.

Inhibition Assays for Thrombin, Factor Xa, and Other Serine Proteases. The test compounds were assayed in vitro for their inhibitory activity toward thrombin, fXa, and other serine proteases, by determining the hydrolysis rates of the synthetic chromogenic substrates monitored at 405 nm. Enzymes and substrates were used as follows (final concentrations): 0.41 unit·mL^{-1} bovine thrombin from Sigma−Aldrich (Milan, Italy) and 50 μM S-2238 (D-Phe-Pip-Arg-*p*-NA) from Chromogenix AB Instrumentation Laboratories; 0.5 nM purified human thrombin and 30 μM S-2238; 4 nM human factor Xa and 0.04 μM S-2765 (Z-D-Arg-Gly-Arg-*p*-NA) from Chromogenix AB-Instrumentation Laboratories (Milan, Italy); 30 nM human recombinant factor VIIa (reconstituted with 0.2 mL of deionized water) and 1 mM Spectrozyme fVIIa from American Diagnostics (Stamford, CT); 0.4 μg·mL^{-1} bovine α-chymotrypsin and 185 μM *N*-succinyl-Ala-Ala-Pro-Phe-*p*-NA from Sigma−Aldrich; 2 nM bovine pancreas trypsin from Calbiochem (Darmstadt, Germany) and 4 mM S-2238; 5 nM human neutrophil leukocyte elastase and 660 μM *N*-(methoxysuccinyl)-Ala-Ala-Pro-Val-*p*-NA from Sigma−Aldrich. Purified human thrombin was obtained as previously reported.[54] Wild-type prothrombin was activated by Taipan snake venom (in 50 mM Tris-HCl, 150 mM NaCl, and 2 mM $CaCl_2$), and the generated thrombin was purified by cation-exchange HPLC. Sodium dodecyl sulfate−polyacrylamide gel electrophoresisE of pooled chromatographic peaks was carried out on 4−20% gradient gels under both reducing (5% β-mercaptoethanol) and nonreducing conditions. The thrombin concentration was measured spectrophotometrically at 280 nm, by use of an extinction coefficient (0.1%) equal to 1.83. The active-site titration was carried out spectrophotometrically, and the purified enzyme was immediately aliquoted and frozen at −80 °C until use. All buffer salts were purchased from Sigma−Aldrich. Enzyme solutions were incubated with DMSO solutions of the test inhibitors (DMSO did not exceed 1%) in various concentrations (0.1−100 nM or 0.1−100 μM), before the respective chromogenic substrates were added to initiate the enzyme kinetics. Kinetic studies were performed at pH 8.0 (10 mM Tris buffer, 150 mM NaCl, and 0.1% PEG6000) for bovine and human fIIa and fXa and at pH 7.5 (50 mM Tris buffer and 50 mM $CaCl_2$) for α-chymotrypsin, recombinant human fVIIa, pancreas bovine trypsin, and human leukocyte elastase. Kinetics for human thrombin, recombinant human fVIIa, pancreas bovine trypsin, and human leukocyte elastase (200 mM Tris buffer, 150 mM NaCl, and 0.1% PEG6000, pH 7.5), were performed by monitoring the absorbance increase at 405 nm and 25 °C with a microplate Bio-Rad spectrophotometer. The enzyme solution (50 μL) and buffer (50 μL) were mixed with 2 μL of DMSO solution containing the test compound or DMSO alone as the control and incubated (15 min for fVIIa, 30 min for trypsin, and 10 min for elastase). Reactions were initiated by adding 100 μL of substrate solutions, and the increase in absorbance was monitored for 5 min. Initial velocities were determined, and the concentrations of the inhibitors required to diminish the control velocity by 50% (IC_{50}) were calculated by nonlinear (sigmoidal) regression. At least three independent IC_{50} values were determined to calculate inhibition constants (K_i) by use of the Cheng−Prusoff equation.[55]

In Vitro Plasma Clotting Time Assays. Clotting time of the test compounds, namely activated partial thromboplastin time (aPTT), was measured on a coagulometer (Behnk Electronic, Norderstedt, Germany) and compared with those from human control plasma. Pooled lyophilized human plasma (100 μL; Futura Systems, Formello, Rome, Italy) was incubated for 3 min at 37 °C with test compound solution (10 μL) or solvent (DMSO maximum of 1%), followed by the addition of aPTT reagent (100 μL) and 0.025 M $CaCl_2$ (100 μL; Futura Systems) to trigger clot formation. Each measurement was performed in triplicate, and the concentration of test compound that caused 2-fold prolongation of the basal clotting times ($aPTT_2$) was calculated from each individual concentration−response curve.

Ex Vivo Anticoagulant Assays in Mice. Ex vivo anticoagulant assays ($aPTT_2$) were performed in agreement with the Italian Law on Animal Care 116/1992 and EEC/609/86, and all efforts were made to minimize the number of animals used. CD1 male mice (Harlan Laboratories) weighing 25−35 g were used. The mice were housed under standard laboratory conditions with open access to standard food and tap water. After overnight fasting, mice were anesthetized by intraperitoneal injection with urethane (1.2 g·kg^{-1}), and test compound **13b**, suspended in a 0.5% methylcellulose solution, was administered orally at concentration 100 mg·kg^{-1} by use of a gastric tube (FTP-20−30, InstechLabs). At 1 and 2 h after test compound administration, blood (0.2 mL) was collected from the inferior vena cava into syringes containing sodium citrate (3.8% v/v). Platelet-poor plasma was then prepared by centrifugation for 20 min at 1200*g* to measure $aPTT_2$. Data (mean ± SEM) were compared with those of the vehicle group. One-way analysis of variance (ANOVA) and multiple comparison tests (Dunnett's test) were performed by use of a standard statistical package. *P* values less than 0.05 were considered statistically significant.

■ ASSOCIATED CONTENT

Supporting Information

Analytical data (IR, NMR, MS) and elemental analyses (C, H, N) for all newly characterized intermediates and test compounds; additional text, three tables, and two figures with X-ray crystal data for **13b**. This material is available free of charge via the Internet at http://pubs.acs.org. The crystal structure of compound **13b** has been deposited in the Cambridge Crystallographic Data Centre (CCDC); http://www.ccdc.cam.ac.uk (deposition code 959986).

■ AUTHOR INFORMATION

Corresponding Author

*Phone +39-080-5442781; fax +39-080-5442230; e-mail cosimodamiano.altomare@uniba.it.

Present Addresses

⊥(F.F.) Farmalabor s.r.l., Via Pozzillo, II Trav. Z.I., 76012 Canosa di Puglia, Italy.

▽(G.L.) Drug Design & Discovery, Aptuit, via A. Fleming, 37135 Verona, Italy.

Notes

The authors declare no competing financial interest.

■ ACKNOWLEDGMENTS

We are grateful to Professor Raimondo De Cristofaro (Catholic University School of Medicine, Rome, Italy), for his helpful collaboration in biological data interpretation, as well as for assistance in the inhibition assays with human serine proteases, and we thank Dr. Brunella Maria Aresta (Istituto di

Cristallografia, Consiglio Nazionale delle Ricerche, Bari, Italy) for her contribution in crystallographic analysis. Financial support by the Italian Ministry for Education Universities and Research (MIUR, Rome, Italy; PRIN 2007, Grant 2007T9HTFB_003) is acknowledged.

ABBREVIATIONS USED

αCT, α-chymotrypsin; ADMET, adsorption, distribution, metabolism, excretion, and toxicity; ADP, adenosine 5′-diphosphate; aPTT, activated partial thromboplastin time; ATIII, antithrombin III; DIAD, diisopropyilazodicarboxylate; DIPEA, *N*,*N*-diisopropylethylamine; DMSO, dimethyl sulfoxide; DTI, direct thrombin inhibitor; DVT, deep venous thrombosis; ESIMS, electrospray ionization mass spectrometry; fIIa, thrombin; fVIIa, activated factor VII; fXa, activated factor X; HDM, hexadecane membrane; HILIC, hydrophilic interaction liquid chromatography; HIT, heparin-induced thrombocytopenia; LE, human leukocyte elastase; LMWHs, low molecular weight heparins; PAMPA, parallel artificial membrane permeability assay; P_e, effective permeability; PE, pulmonary embolism; PSA, polar surface area; SASA, solvent-accessible surface area; TBTU, *O*-(benzotriazol-1-yl)-*N*,*N*,*N*′,*N*′-tetramethyluronium tetrafluoroborate; Try, trypsin; UFHs, unfractionated heparins; VTE, venous thromboembolism

REFERENCES

(1) (a) Macmanaman, N. Triggers, targets and treatment for thrombosis. *Nature* **2008**, *451*, 914−918. (b) Beckman, M. G.; Hooper, W. C.; Critchley, S. E.; Ortel, T. L. Venous thromboembolism: a public health concern. *Am. J. Prev. Med.* **2010**, *38* (4S), S495−S501. (c) Chaudhry, F. S.; Schneck, M. J.; Morales-Vidal, S.; Javaid, F.; Ruland, S. Prevention of venous thromboembolism in patients with hemorrhagic stroke. *Top. Stroke Rehabil.* **2013**, *20*, 108−115.

(2) Alban, S. Pharmacological strategies for inhibition of thrombin activity. *Curr. Pharm. Des.* **2008**, *14*, 1152−1175.

(3) Haas, S. New oral Xa and IIa inhibitors: updates on clinical trial results. *J. Thromb. Thrombolysis* **2008**, *25*, 52−60.

(4) Hirsch, J.; Dalen, J. E.; Anderson, D. R.; Poller, L.; Bussey, H.; Ansell, J.; Deykin, D. Oral anticoagulants: mechanism of action, clinical effectiveness, and optimal therapeutic range. *Chest* **2001**, *119*, 8S−21S.

(5) Hirsch, J.; Raschke, R. Heparin and low-molecular-weight heparin: the seventh ACCP conference on antithrombotic and thrombolytic therapy. *Chest* **2004**, *126*, 188S−203S.

(6) (a) Schwarz, R. P. The preclinical and clinical pharmacology of Novastan (Argatroban). In *New Anticoagulants for the Cardiovascular Patient*; Pifarre, R., Ed.; Hanley and Belfus Inc.: Philadelphia, PA, 1997; pp 231−249. (b) Schwienhorst, A. Direct thrombin inhibitors: A survey of recent developments. *Cell. Mol. Life Sci.* **2006**, *63*, 2773−2791.

(7) Linusson, A.; Gottfries, J.; Olsson, T.; Ornskov, E.; Folestad, S.; Nordèn, B.; Wold, S. Statistical molecular design, parallel synthesis, and biological evaluation of a library of thrombin inhibitors. *J. Med. Chem.* **2001**, *44*, 3424−3439.

(8) Coughlin, S. R.; Vu, T.-K. H.; Hung, D. T.; Wheaton, V. I. Characterization of a functional thrombin receptor. *J. Clin. Invest.* **1992**, *89*, 351−355.

(9) Van Obbergghen-Schilling, E.; Pouysséggur, J. Signaling pathways of the thrombin receptor. *Thromb. Haemostasis* **1993**, *70*, 163−167.

(10) Weitz, J.; Crowther, M. Direct thrombin inhibitors. *Thromb. Res.* **2002**, *106*, V275−V284.

(11) Weitz, J. I. A novel approach to thrombin inhibition. *Thromb. Res.* **2003**, *109* (Suppl. 1), S17−S22.

(12) Weitz, J.; Leslie, B.; Hudoba, M. Thrombin binds to soluble fibrin degradation products where it is protected from inhibition by heparin-antithrombin but susceptible to inactivation by antithrombin-independent inhibitors. *Circulation* **1998**, *97*, 544−552.

(13) Dhillon, S. Argatroban: A review of its use in the management of heparin-induced thrombocytopenia. *Am. J. Cardiovasc. Drugs* **2009**, *9*, 261−282.

(14) Sorbera, L. A.; Bayes, M. C. J.; Silvestre, J. Melagatran and ximelagatran. *Drugs Future* **2001**, *26*, 1155−1170.

(15) AstraZeneca decides to withdraw Exanta. http://www.astrazeneca.com/media/latest-press-releases/2006/5217?itemId=3891692, 2006.

(16) Hauel, N. H.; Nar, H.; Priepke, H.; Ries, U.; Stassen, J.-M.; Wienen, W. Structure-based design of novel potent nonpeptide thrombin inhibitors. *J. Med. Chem.* **2002**, *45*, 1757−1766.

(17) (a) Stangier, J.; Rathgen, K.; Stahle, H.; Gansser, D.; Roth, W. The pharmacokinetics, pharmacodynamics and tolerability of dabigatran etexilate, a new oral direct thrombin inhibitor, in healthy male subjects. *Br. J. Clin. Pharmacol.* **2007**, *64*, 292−303. (b) Eriksson, B. I.; Dahl, O. E.; Rosencher, N.; Kurth, A. A.; van Dijk, C. N.; Frostick, S. P.; Prins, M. H.; Hettiarachchi, R.; Hantel, S.; Schnee, J.; Büller, H. R. Dabigatran etexilate versus enoxaparin for prevention of venous thromboembolism after total hip replacement: a randomised, double-blind, non-inferiority trial. *Lancet* **2007**, *370*, 949−956. (c) Larsen, T. B.; Rasmussen, L. H.; Skjøth, F.; Due, K. M.; Callréus, T.; Rosenzweig, M.; Lip, G. Y. Efficacy and safety of dabigatran etexilate and warfarin in "real-world" patients with atrial fibrillation: a prospective nationwide cohort study. *J. Am. Coll. Cardiol.* **2013**, *61*, 2264−2273.

(18) (a) de Candia, M.; Summo, L.; Carrieri, A.; Altomare, C.; Nardecchia, A.; Cellamare, S.; Carotti, A. Investigation of platelet aggregation inhibitory activity by phenyl amides and esters of piperidinecarboxylic acids. *Bioorg. Med. Chem.* **2003**, *11*, 1439−1450. (b) De Marco, A.; de Candia, M.; Carotti, A.; Cellamare, S.; De Candia, E.; Altomare, C. Lipophilicity-related inhibition of blood platelet aggregation by nipecotic acid anilides. *Eur. J. Pharm. Sci.* **2004**, *22*, 153−164.

(19) de Candia, M.; Liantonio, F.; Carotti, A.; De Cristofaro, R.; Altomare, C. Fluorinated benzyloxyphenyl piperidine-4-carboxamides with dual function against thrombosis: Inhibitors of factor Xa and platelet aggregation. *J. Med. Chem.* **2009**, *52*, 1018−1028.

(20) (a) Friesner, R. A.; Banks, J. L.; Murphy, R. B.; Halgren, T. A.; Klicic, J. J.; Mainz, D. T.; Repasky, M. P.; Knoll, E. H.; Shelley, M.; Perry, J. K.; Shaw, D. E.; Francis, P.; Shenkin, P. S. Glide: A new approach for rapid, accurate docking and scoring. 1. Method and assessment of docking accuracy. *J. Med. Chem.* **2004**, *47*, 1739−1749. (b) Halgren, T. A.; Murphy, R. B.; Friesner, R. A.; Beard, H. S.; Frye, L. L.; Pollard, W. T.; Banks, J. L. Glide: A new approach for rapid, accurate docking and scoring. 2. Enrichment factors in database screening. *J. Med. Chem.* **2004**, *47*, 1750−1759. (c) Friesner, R. A.; Murphy, R. B.; Repasky, M. P.; Frye, L. L.; Greenwood, J. R.; Halgren, T. A.; Sanschagrin, P. C.; Mainz, D. T. Extra precision Glide: Docking and scoring incorporating a model of hydrophobic enclosure for protein-ligand complexes. *J. Med. Chem.* **2006**, *49*, 6177−6196.

(21) Engh, R. A.; Brandstetter, H.; Sucher, G.; Eichinger, A.; Baumann, U.; Bode, W.; Huber, R.; Poll, T.; Rudolph, R.; Von der Saal, W. Enzyme flexibility, solvent and weak interactions characterize thrombin-ligand interactions: implications for drug design. *Structure* **1996**, *4*, 1353−1362.

(22) Faller, B. Artificial membrane assays to assess permeability. *Curr. Drug Metab.* **2008**, *9*, 886−892.

(23) Ottaviani, G.; Martel, S.; Escarala, C.; Nicolle, E.; Carrupt, P.-A. The PAMPA technique as a HTS tool for partition coefficients determination in different solvent/water system. *Eur. J. Pharm. Sci.* **2008**, *35*, 68−75.

(24) Batt, A. R.; Heeney, C.; Marguerite, S. Diazepinyl(piperidin-4-yl)methanone derivatives as vasopressin receptor V1a antagonists and their preparation and use for the treatment of diseases. World Patent WO2010097576 (A8), 2011.

(25) Johnson, P. S.; Ryckmans, T.; Bryans, J.; Beal, D. M.; Dacka, K. N.; Feeder, N.; Harrison, A.; Lewis, M.; Mason, H. J.; Mills, J.; Newman, J.; Pasquinet, C.; Rawson, D. J.; Roberts, L. R.; Russell, R.;

Spark, D.; Stobie, A.; Underwood, T. J.; Ward, R.; Wheeler, S. Discovery of PF-184563, a potent and selective V1a antagonist for the treatment of dysmenorrhoea. The influence of compound flexibility on microsomal stability. *Bioorg. Med. Chem. Lett.* **2011**, *21*, 5684−5687.

(26) Guendouz, F.; Jacquier, R.; Verducci, J. Polymer bound 4-dialkylamino pyridines: Synthesis, characterization and catalytic efficiency. *Tetrahedron* **1988**, *44*, 7095−7108.

(27) Cruege, F.; Girault, G.; Coustal, S.; Lascombe, J.; Rumpf, P. Basic properties of dimethylamino derivatives of pyridine and pyrimidine. *Bull. Soc. Chim. France* **1970**, *11*, 3889−3894.

(28) Von der Saal, W.; Kucznierz, R.; Leinert, H.; Engh, R. A. Derivatives of 4-aminopyridine as selective thrombin inhibitors. *Bioorg. Med. Chem. Lett.* **1997**, *7*, 1283−1288.

(29) Engh, R. A.; Brandstetter, H.; Sucher, G.; Eichinger, A.; Baumann, U.; Bode, W.; Huber, R.; Poll, T.; Rudolph, R.; Von der Saal, W. Enzyme flexibility, solvent and weak interactions characterize thrombin-ligand interactions: implications for drug design. *Structure* **1996**, *4*, 1353−1362.

(30) Wohnsland, F.; Faller, B. High-throughput permeability pH profile and high-throughput alkane/water log *P* with artificial membranes. *J. Med. Chem.* **2001**, *44*, 923−930.

(31) Fischer, H.; Kansy, M.; Avdeef, A.; Senner, F. Permeation of permanently positive charged molecules through artificial membranes: Influence of physico-chemical properties. *Eur. J. Pharm. Sci.* **2007**, *31*, 32−42.

(32) Olsen, J. A.; Banner, D. W.; Seiler, P.; Obst-sandr, U.; D'Arcy, A.; Stihle, M.; Mueller, K.; Diederich, F. A fluorine scan of thrombin inhibitors to map the fluorophilicity/fluorophobicity of an enzyme active site: Evidence for C-F···C=O interactions. *Angew. Chem., Int. Ed.* **2003**, *42*, 2507−2511.

(33) Hoffmann-Roeder, A.; Schweizer, E.; Egger, J.; Seiler, P.; Obst-Sander, U.; Wagner, B.; Kansy, M.; Banner, D. W.; Diederich, F. Mapping the fluorophilicity of a hydrophobic pocket: Synthesis and biological evaluation of tricyclic thrombin inhibitors directing fluorinated alkyl groups into P pocket. *ChemMedChem* **2006**, *1*, 1205−1215.

(34) Obst, U.; Banner, D. W.; Weber, L.; Diederich, F. Molecular recognition at the thrombin active site: structure-based design and synthesis of potent and selective thrombin inhibitors and the X-ray crystals structure of two thrombin-inhibitor complexes. *Chem. Biol.* **1997**, *4*, 287−295.

(35) Cummings, M. D.; DesJarlais, R. L.; Gibbs, A. C.; Mohan, V.; Jaeger, E. P. Comparison of automated docking programs as virtual screening tools. *J. Med. Chem.* **2005**, *48*, 962−976.

(36) Bytheway, I.; Cochran, S. Validation of molecular docking calculations involving FGF-1 and FGF-2. *J. Med. Chem.* **2004**, *47*, 1683−1693.

(37) Enyedy, I. J.; Egan, W. J. Can we use docking and scoring for hit-to-lead optimization? *J. Comput.-Aided Mol. Des.* **2008**, *22*, 161−168.

(38) Muley, L.; Baum, B.; Smolinski, M.; Freindorf, M.; Heine, A.; Klebe, G.; Hangauer, D. G. Enhancement of hydrophobic interactions and hydrogen bond strength by cooperativity: Synthesis, modeling, and molecular dynamics simulation of a congeneric series of thrombin inhibitors. *J. Med. Chem.* **2010**, *53*, 2126−2135.

(39) Lévesque, S.; St-Denis, Y.; Bachand, B.; Préville, P.; Leblond, L.; Winocour, P. D.; Edmunds, J. J.; Rubin, J. R.; Siddiqui, M. A. Novel bicyclic lactam inhibitors of thrombin: potency and selectivity optimization through P1 residues. *Bioorg. Med. Chem. Lett.* **2001**, *11*, 3161−3164.

(40) Hanessian, S.; Therrien, E.; van Otterlo, W. A.; Bayrakdarian, M.; Nilsson, I.; Fjellström, O.; Xue, Y. Phenolic P2/P3 core motif as thrombin inhibitors: Design, synthesis, and X-ray co-crystal structure. *Bioorg. Med. Chem. Lett.* **2006**, *16*, 1032−1036.

(41) Tucker, T. J.; Lumma, W. C.; Lewis, S. D.; Gardell, S. J.; Lucas, B. J.; Baskin, E. P.; Woltmann, R.; Lynch, J. J.; Lyle, E. A.; Appleby, S. D.; Chen, I.-W.; Dancheck, K. B.; Vacca, J. P. Potent noncovalent thrombin inhibitors that utilize the unique amino acid D-dicyclohexylalanine in the P3 position. Implications on oral bioavailability and antithrombotic efficacy. *J. Med. Chem.* **1997**, *40*, 1565−1569.

(42) Remko, M. Molecular structure, lipophilicity, solubility, absorption, and polar surface area of novel anticoagulant agents. *J. Mol. Struct. Theochem.* **2009**, *916*, 76−85.

(43) Bard, B.; Carrupt, P.-A.; Martel, S. Lipophilicity of basic drugs measured by hydrophilic interaction chromatography. *J. Med. Chem.* **2009**, *52*, 3416−3419.

(44) Lopopolo, G.; Fiorella, F.; de Candia, M.; Nicolotti, O.; Martel, S.; Carrupt, P.-A.; Altomare, C. Biarylmethoxy isonipecotanilides as potent and selective inhibitors of blood coagulation factor Xa. *Eur. J. Pharm. Sci.* **2011**, *42*, 180−191.

(45) Burla, M. C.; Caliandro, R.; Camalli, M.; Carrozzini, B.; Cascarano, G.l.; Giacovazzo, C.; Mallamo, M.; Mazzone, A.; Polidori, G.; Spagna, R. SIR2011: A new package for crystal structure determination and refinement. *J. Appl. Crystallogr.* **2012**, *45*, 357−361.

(46) Sheldrick, G. M. A short history of SHELX. *Acta Crystallogr.* **2008**, *A64*, 112−122.

(47) Farrugia, L. J. ORTEP-3 for Windows: A version of ORTEP-III with a graphical user interface (GUI). *J. Appl. Crystallogr.* **1997**, *30*, 565.

(48) (a) Avdeef, A. pH-metric log P. Part 1. Difference plots for determining ion-pair octanol-water partition coefficients of multiprotic substances. *Quant. Struct.-Act. Relat.* **1992**, *11*, 510−517. (b) Avdeef, A. J. pH-Metric log P. II. Refinement of partition coefficients and ionization constants of multiprotic substances. *Pharm. Sci.* **1993**, *82*, 183−190. (c) Avdeef, A.; Box, K. J.; Comer, J. E. A.; Hibbert, C.; Tam, K. Y. pH-metric logP 10. Determination of liposomal membrane-water partition coefficients of ionizable drugs. *Pharm. Res.* **1998**, *15*, 209−215.

(49) Vecchia, B. E.; Bunge, A. *Transdermal Drug Delivery*; Marcel Dekker: New York, 2003; pp 57−141.

(50) Ruell, J. A.; Tsinman, K. L.; Avdeef, A. PAMPA: A drug absorption *in vitro* model 5. Unstirred water layer in iso-pH mapping assays and pKaflux-optimized design (pOD-PAMPA). *Eur. J. Pharm. Sci.* **2003**, *20*, 393−402.

(51) Avdeef, A.; Strafford, M.; Block, E.; Balogh, M. P.; Chambliss, W.; Khan, I. Drug absorption *in vitro* model: filter-immobilized artificial membranes 2. Studies of the permeability properties of lactones in *Piper methysticum* Forst. *Eur. J. Pharm. Sci.* **2001**, *14*, 271−280.

(52) Bowers, K. J.; Chow, E.; Xu, H.; Dror, R. O.; Eastwood, M. P.; Gregersen, B. A.; Klepeis, J. L.; Kolossváry, I.; Moraes, M. A.; Sacerdoti, F. D.; Salmon, J. K.; Shan, Y.; Shaw, D. E. Scalable algorithms for molecular dynamics simulations on commodity clusters. In *Proceedings of the ACM/IEEE Conference on Supercomputing (SC06)*, Tampa, Florida, November 11−17, 2006. DOI: 10.1145/1188455.1188544.

(53) Humphrey, W.; Dalke, A.; Schulten, K. VDM: visual molecular dynamics. *J. Mol. Graphics* **1996**, *14*, 33−38.

(54) De Cristofaro, R.; Akhavan, S.; Altomare, C.; Carotti, A.; Peyvandi, F.; Mannucci, P. M. A natural prothrombin mutant reveals an unexpected influence of A-chain structure on the activity of human alpha-thrombin. *J. Biol. Chem.* **2004**, *279*, 13035−13043.

(55) Cheng, Y.; Prusoff, W. H. Relation between the inhibition constant K1) and the concentration of inhibitor which causes fifty per cent inhibition (I_{50}) of an enzymic reaction. *Biochem. Pharmacol.* **1973**, *22*, 3099−3108.

(56) *Schrodinger Suite 2011*; Schrodinger Inc., LLC, New York, 2011.